

**DISCLAIMER**

DE88 015116

This report was prepared as an account of work sponsored by an agency of the United States Government. Neither the United States Government nor any agency thereof, nor any of their employees, makes any warranty, express or implied, or assumes any legal liability or responsibility for the accuracy, completeness, or usefulness of any information, apparatus, product, or process disclosed, or represents that its use would not infringe privately owned rights. Reference herein to any specific commercial product, process, or service by trade name, trademark, manufacturer, or otherwise does not necessarily constitute or imply its endorsement, recommendation, or favoring by the United States Government or any agency thereof. The views and opinions of authors expressed herein do not necessarily state or reflect those of the United States Government or any agency thereof.

**TMI-2 STANDING FUEL ROD SEGMENTS:  
PRELIMINARY EXAMINATION REPORT**

Douglas W. Akers  
Malcolm L. Russell

Published August 1987

EG&G Idaho, Inc.  
Idaho Falls, Idaho 83415

Prepared for the  
U.S. Department of Energy  
Idaho Operations Office  
Under DOE Contract No. DE-AC07-76ID01570

**MASTER**

## ABSTRACT

Six fuel rod segments were obtained from partially intact fuel assemblies still standing in the core of the damaged Three Mile Island Unit 2 reactor. The segments were subjected to neutron radiography, gamma spectroscopy, and visual and photographic examination to evaluate the necessity of performing additional metallurgical and radiochemical analyses. It was determined that the fuel rod segments were only slightly damaged during the accident sequence and not useful for further destructive examination by the TMI-2 Accident Evaluation Program except for use as possible comparison samples in other TMI-2 core component examination programs.

## CONTENTS

ABSTRACT .....	ii
1. INTRODUCTION .....	1
1.1 Purpose .....	1
1.2 Background .....	1
2. SAMPLE HISTORY .....	4
2.1 Fuel Rod Design Characteristics .....	4
2.2 TMI-2 Accident and Recovery Period Environment .....	4
2.3 Segment Locations in the Core .....	9
2.4 Segment Acquisition, Packaging, and Shipping .....	16
2.4.1 Retrieval from the Core .....	16
2.4.2 Packaging and Shipping .....	16
3. EXAMINATION PLAN AND ANALYTICAL METHODS .....	18
4. EXAMINATION RESULTS .....	20
4.1 Neutron Radiography .....	20
4.2 Gamma Spectroscopy .....	24
4.3 Visual and Photographic Examinations .....	32
5. OBSERVATIONS/CONCLUSIONS .....	45
6. REFERENCES .....	47
APPENDIX A--GAMMA SPECTROSCOPY ANALYSIS RESULTS .....	A-1

## FIGURES

1. Cross-sectional view of a representative, prepressurized fuel rod from the TMI-2 core .....	6
2. Hypothesized end state of the TMI-2 core and reactor vessel .....	7
3. Topographical, cross-sectional map of the TMI-2 core cavity .....	8

4.	Locations of the standing fuel rod segments retrieved from the TMI-2 core .....	10
5.	View of the side of the TMI-2 core cavity, showing the fuel assembly at core position L1 .....	12
6.	View of the side of the TMI-2 core cavity, showing the fuel assembly at core position N2 .....	13
7.	View of the side of the TMI-2 core cavity, showing the fuel assembly at core position M2 .....	14
8.	Neutron radiographs of Segment 1 (core position L1, rod position B10, at the transition region) and Segment 2 (core position L1, rod position B10, near the top of the rod) .....	21
9.	Neutron radiographs of Segment 3 (core position N2, rod position N1) and Segment 4 (core position M2, rod position R15) .....	22
10.	Neutron radiographs of Segment 5 (core position M2, rod position R13, upper segment) and Segment 6 (core position M2, rod position R13, lower segment) .....	23
11.	Gross Cs-137 distribution along Segment 5 .....	26
12.	Gross Sb-125 distribution along Segment 5 .....	26
13.	Ru-106 distribution along Segment 5 .....	27
14.	Ce-144 distribution along Segment 5 .....	27
15.	Eu-154 distribution along Segment 5 .....	28
16.	Co-60 distribution along Segment 5 .....	28
17.	Side view of Segment 1 inside the container tube, showing the transition region at the right end. A new segment of fuel rod cladding is shown above for comparison .....	33
18.	Side view of Segment 1 inside the container tube, showing the transition region at the right end. A new segment of fuel rod cladding inside a container tube is shown above for comparison .....	33
19.	Side view of Segment 2, after sectioning removal of the lower end deformed by the TMI-2 defueling shear tool. A new segment of fuel rod cladding is shown above for comparison .....	34
20.	View of Segment 2, showing the top end deformed by the TMI-2 defueling shear tool and the top end of the zircaloy spacer sleeve, which was between the fuel pellet stack holddown spring and the pellet stack. A new segment of fuel rod cladding is shown at the right for comparison .....	34

21.	Bottom end view of Segment 2, after sectioning removal of both ends deformed by the TMI-2 defueling shear tool. Removed ends are shown below, and a new segment of fuel rod cladding is shown for comparison .....	35
22.	Side view of Segment 3, after sectioning removal of both ends deformed by the TMI-2 defueling shear tool. A new segment of fuel rod cladding is shown above for comparison .....	35
23.	Top end view of Segment 3, after sectioning removal of the top end deformed by the TMI-2 defueling shear tool. A new segment of fuel rod cladding is shown at the right for comparison .....	36
24.	Bottom end view of segment 3, after sectioning removal of both ends deformed by the TMI-2 defueling shear tool. Removed ends are shown below and a new segment of fuel rod cladding is shown at the right for comparison .....	37
25.	Bottom end view of Segment 3, after sectioning removal of both ends deformed by the TMI-2 defueling shear tool. Removed ends are shown below, and a new segment of fuel rod cladding is shown at the right for comparison .....	38
26.	Side view of Segment 4, showing both ends deformed by the TMI-2 defueling shear tool. A new segment of fuel rod cladding is shown above for comparison .....	39
27.	View of Segment 4, showing the top end deformed by the TMI-2 defueling shear tool. A new segment of fuel rod cladding is shown at the left for comparison .....	39
28.	View of Segment 4, showing the bottom end deformed by the TMI-2 defueling shear tool. A new segment of fuel rod cladding is shown at the left for comparison .....	40
29.	Side view of Segment 5, showing both ends deformed by the TMI-2 defueling shear tool. A new segment of fuel rod cladding is shown above for comparison .....	40
30.	View of Segment 5, showing the top end deformed by the TMI-2 defueling shear tool. A new segment of fuel rod cladding is shown at the left for comparison .....	41
31.	View of Segment 5, showing the bottom end deformed by the TMI-2 defueling shear tool. A new segment of fuel rod cladding is shown at the left for comparison .....	42
32.	Side view of Segment 6, after sectioning removal of the lower end deformed by the TMI-2 defueling shear tool. A new segment of fuel rod cladding is shown above for comparison .....	43

33.	View of Segment 6, showing the top end deformed by the TMI-2 defueling shear tool. The removed end is shown below, and a new segment of fuel rod cladding is shown at the right for comparison .....	43
34.	View of Segment 6, after sectioning removal of the bottom end deformed by the TMI-2 defueling shear tool. The removed end is shown below, and a new segment of fuel rod cladding is shown at the right for comparison .....	44
A-1.	Gamma spectrometry system configuration .....	A-3

TABLES

1.	TMI-2 fuel rod design data .....	5
2.	Fuel rod segment characteristics .....	25
3.	ORIGEN2 calculated burnup ranges at segment locations .....	30
4.	Comparison of measured and ORIGEN2 calculated radionuclide concentrations at three segment locations.....	31
A-1.	Calibration measurements using the Europium-152 standard .....	A-4
A-2.	Calibration efficiency data .....	A-5
A-3.	Gamma spectroscopy data for Segment 5 .....	A-6
A-4.	Gamma Spectroscopy data for Segments 1, 2, 3, 4, and 6 .....	A-7
A-5.	Individual radionuclide efficiencies at defined energies .....	A-9

TMI-2 STANDING FUEL ROD SEGMENTS:  
PRELIMINARY EXAMINATION REPORT

1. INTRODUCTION

1.1 Purpose

The principal purpose of the nondestructive examination of the six fuel rod segments obtained from partially intact fuel assemblies still standing in the core of the Three Mile Island Unit 2 (TMI-2) reactor was to evaluate their potential for providing information that may contribute significantly toward understanding the TMI-2 accident. Objectives of the examinations were to (a) evaluate the necessity for performing destructive metallurgical and radiochemical examinations and (b) identify the best locations for removing samples for other analyses.

1.2 Background

Although the March 28, 1979, accident at TMI-2 involved severe damage to the core of the reactor, the accident was determined to have had little effect on the health and safety of the public.<sup>1</sup> However, as a consequence of the severe loss-of-coolant accident close scrutiny has been given various aspects of the regulations concerning the safety of light water reactors, and several major research programs were initiated by organizations concerned with nuclear power safety. As part of these efforts, the U.S. Department of Energy (DOE) established a program to (a) develop the technology necessary to recover the TMI-2 plant from a serious reactor accident, and (b) conduct relevant research on the TMI-2 accident to enhance the understanding of severe fuel damage accidents and nuclear power plant safety.

Other organizations with interests in both plant recovery and acquisition of accident data formally agreed to cooperate with DOE in these areas. These organizations, commonly referred to as the GENO Group--General Public Utilities Nuclear Corporation (GPU Nuclear), Electric Power Research Institute, the U.S. Nuclear Regulatory Commission, and

DOE--are actively involved in both reactor recovery and accident research. At present, DOE is providing a portion of the funds for reactor recovery (in those areas where accident recovery knowledge will be of generic benefit to the U.S. light water reactor industry), as well as the majority of funds for acquiring severe accident technical data (such as obtained from examining the damaged core).

EG&G Idaho, Inc., involvement with the TMI-2 accident has been continuous. Initially, DOE requested that EG&G Idaho collect, analyze, distribute, and preserve significant technical information. Subsequently, this was expanded to include (a) conducting research and development activities intended to effectively exploit the generic research and development challenges at TMI-2, and (b) developing an understanding of the accident sequence-of-events in the areas of core damage and escape of radionuclides (fission products) and materials from the reactor core.

The Sample Acquisition and Examination (SA&E) Program, which is part of the TMI-2 Accident Evaluation Program funded by DOE, is described in References 1 and 2. The SA&E Program includes in situ measurements within the reactor, sample acquisition, and examinations performed by private organizations and state and federal agencies. Some of the data obtained to date indicate the following:

- Temperatures in large regions of the core exceeded the melting temperature (~2200 K) of the fuel cladding, significant fuel liquefaction by molten zircaloy occurred, and evidence of some fuel melting has been observed, indicating temperatures up to 3100 K.
- Some core materials relocated into lower parts of the reactor, leaving a void in the upper core region equivalent to approximately 25% of the original volume. Between ten and twenty metric tons of core and structural materials now are located in the space between the bottom head of the reactor vessel and the elliptical flow distributor.

- Fission product retention in core materials remaining within the core is significant. Fission products relocated outside the core were located primarily in reactor cooling system water, and water and concrete in the Reactor Building basement.

Significant findings from the examinations have resulted in the following: (a) increased technical interest in TMI-2, because the accident represents a severe fuel damage event in full-scale, (b) reconsideration of plans and equipment for defueling the TMI-2 reactor, and (c) expansion of the TMI-2 accident examination plan to determine both the consequences of high temperature interactions between core components and the extent of release from the fuel of the lower volatility fission products.

Examination of the fuel rod segments will provide direct data on localized temperature, fission product retention, material composition, and extent of oxidation. Analysis of these data will provide a basis of comparison for benchmarking core heat-up and fission product transport codes, checking estimates of hydrogen generation, and comparing source term calculations.

## 2. SAMPLE HISTORY

This section presents specific details concerning the design, history, and acquisition of the fuel rod segments, including (a) design characteristics of the TMI-2 fuel rods; (b) the environment that the rods were exposed to during the accident and subsequent 5 years; (c) the original locations of the segments in the core; and (d) acquisition techniques, handling methods, and packaging for shipment to the Idaho National Engineering Laboratory (INEL).

### 2.1 Fuel Rod Design Characteristics

Design data for the TMI-2 fuel rods<sup>3</sup> are summarized in Table 1 of this report.<sup>a</sup> A cross-sectional view of a representative, prepressurized fuel rod from the TMI-2 core is presented in Figure 1.

### 2.2 TMI-2 Accident and Recovery Period Environment

This section briefly describes some of the environmental conditions in the TMI-2 reactor during the accident and subsequent 5 years before acquisition of the fuel rod segments. A more comprehensive description of the accident sequence and its effect on the fuel assemblies still standing at the core periphery in the upper core region is contained in Reference 2.

The end-state of the upper reactor core region, support structures, and reactor vessel, as hypothesized from various examinations and measurements, is shown in Figure 2. A void existed in the upper region of the core that encompassed approximately 25% of the total core volume and extended to the outermost fuel assemblies. Figure 3 is a topographical, cross-sectional map of the sides of the core cavity at the elevations from which the fuel rod segments were obtained.<sup>4</sup> The segments were cut from standing fuel rods at core positions 11, N2, and M2. The rods appear to be representative of intact fuel rods.

---

a. The TMI-2 core was composed of three uranium enrichment zones (1.98, 2.64, and 2.96 wt%). The six fuel rod segments all are of the 2.96-wt% enrichment category.

TABLE 1. 1MI-2 FUEL ROD DESIGN DATA

Parameter	Value	Comments
Geometry	--	Cylindrical
Total length (cm)	389.1	--
Active fuel length (cm)	360	--
Cladding OD (cm)	1.1	--
Cladding ID (cm)	0.94	--
Pellet diameter (cm)	0.93	--
Pellet density (% T.D.) <sup>a</sup>	92.5 ± 1.5	--
Pellet enrichment (wt%)	1.98, 2.64, and 2.96	--
Pellet length (cm)	1.75	--
Pellet dish (vol%)	1.7 ± 0.5	Assumed <sup>b</sup>
Upper plenum length (cm)	20.0 ± 2.5	Assumed <sup>b</sup>
Lower plenum length (cm)	7.5 ± 2.5	Assumed <sup>b</sup>
Fill gas pressure (psia)	465 ± 50, helium	Assumed <sup>b</sup>
Plenum spring volume (cm/cm <sup>3</sup> )	0.20 ± 0.01	Assumed <sup>b</sup>
Spacer diameter (cm)	0.92	--
Spacer length (cm)	1.1	Assumed <sup>b</sup>
Fuel material	Sintered UO <sub>2</sub>	--
Cladding material	Cold-worked Zircaloy-4	--
End plug material	Zircaloy-4	--
Spring material	304 SS	Assumed <sup>b</sup>
Spacer material	ZrO <sub>2</sub>	--
Material weights:		
UO <sub>2</sub> (kg)	1.03	--
Zircaloy-4 (kg)	0.56	--
304 SS (kg)	0.02	Assumed <sup>b</sup>
ZrO <sub>2</sub> (kg)	0.01	--
Total material weight (kg)	3.12	--

a. % T.D. = percent of theoretical density.

b. Based on original design criteria for fuel pellets.

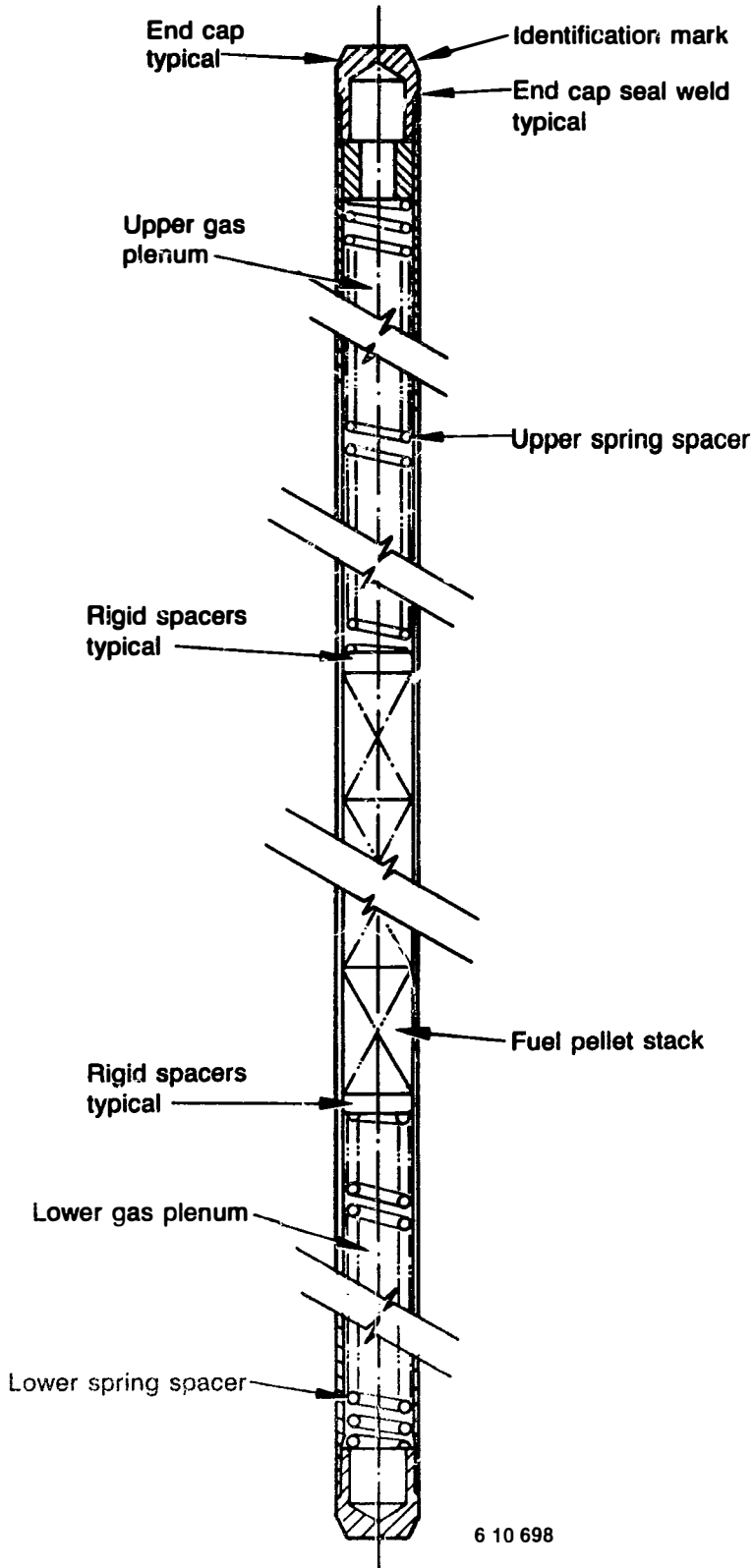
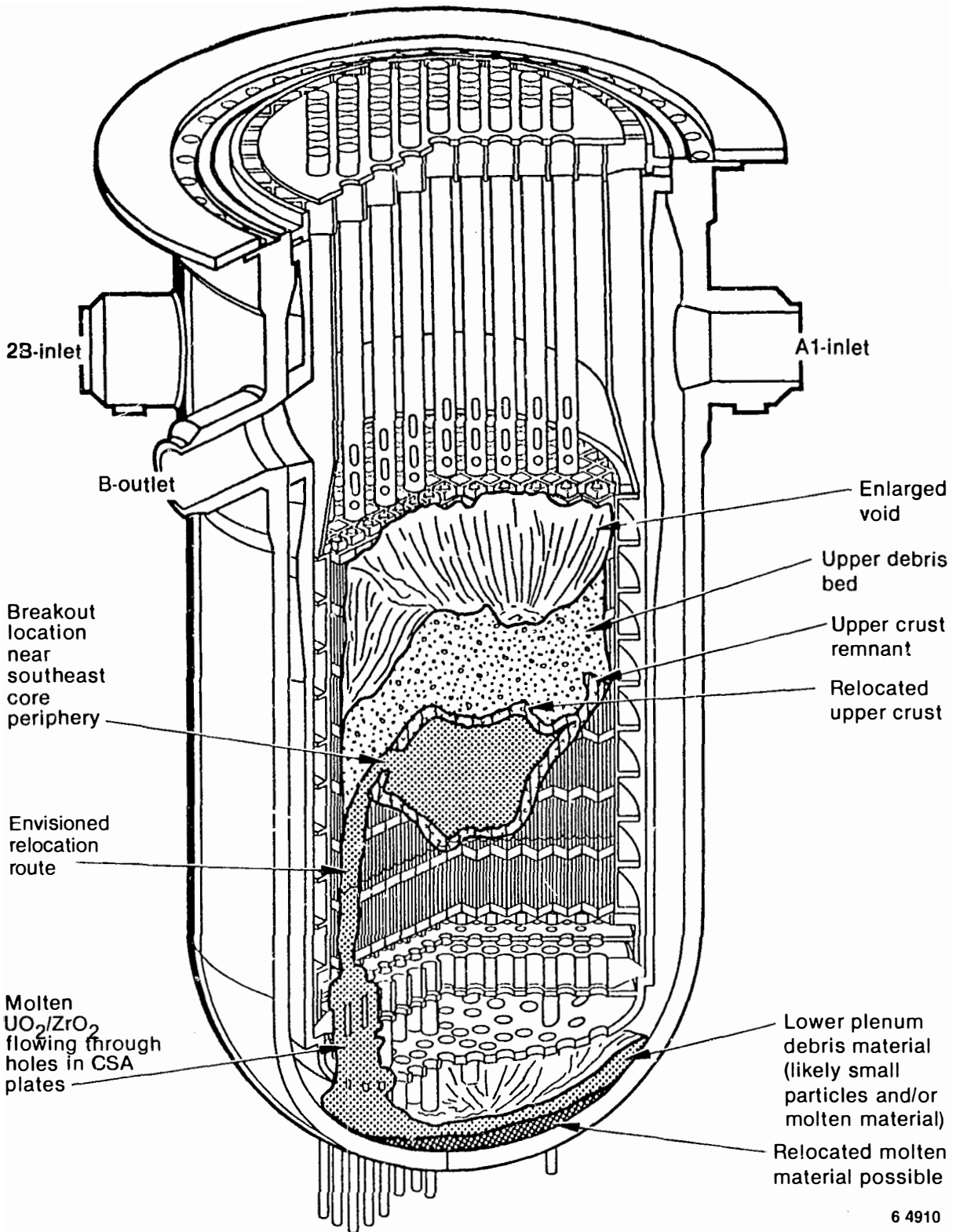


Figure 1. Cross-sectional view of a representative, prepressurized fuel rod from the TMI-2 core.



6 4910

Figure 2. Hypothesized end state of the TMI-2 core and reactor vessel.

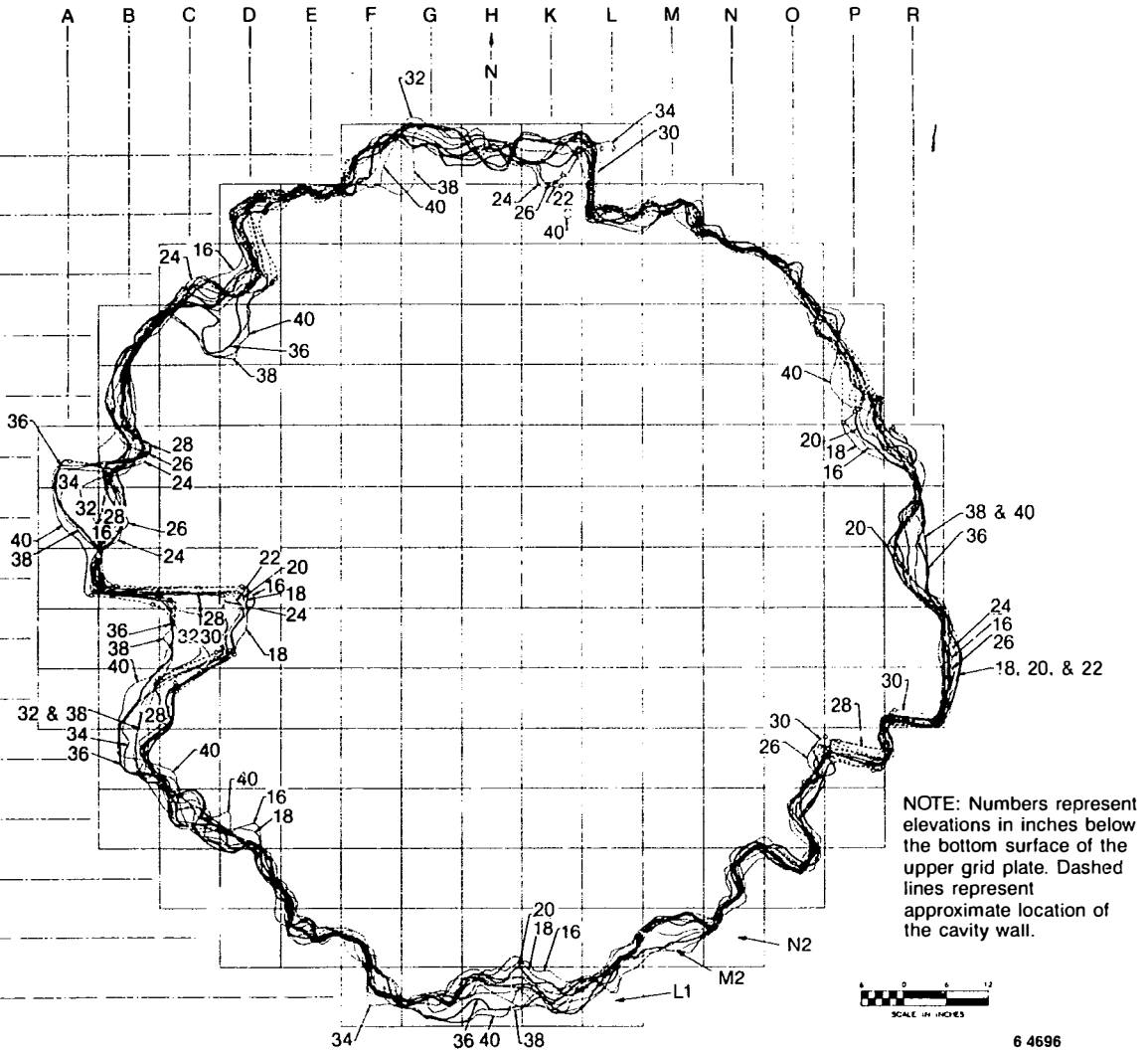


Figure 3. Topographical, cross-sectional map of the IMI-2 core cavity.

A debris bed ranging from 0.6- to about 1.0-m deep was at the bottom of the core cavity. Samples of debris from two locations near the center of the debris bed have been obtained and examined. A hard (impenetrable) layer of material was detected about 1.6 m from the bottom of the core (i.e., near the mid-core elevation) when the debris bed was probed mechanically.

After the accident, the fuel rods remained in the TMI-2 reactor vessel until December 22, 1985 (~5 years). They were submerged in water at ambient temperature and pressure, with the following concentrations:

- pH: 7.5 to 7.7
- Boron: >4350 ppm
- Buffer: sodium hydroxide (1500 ppm).

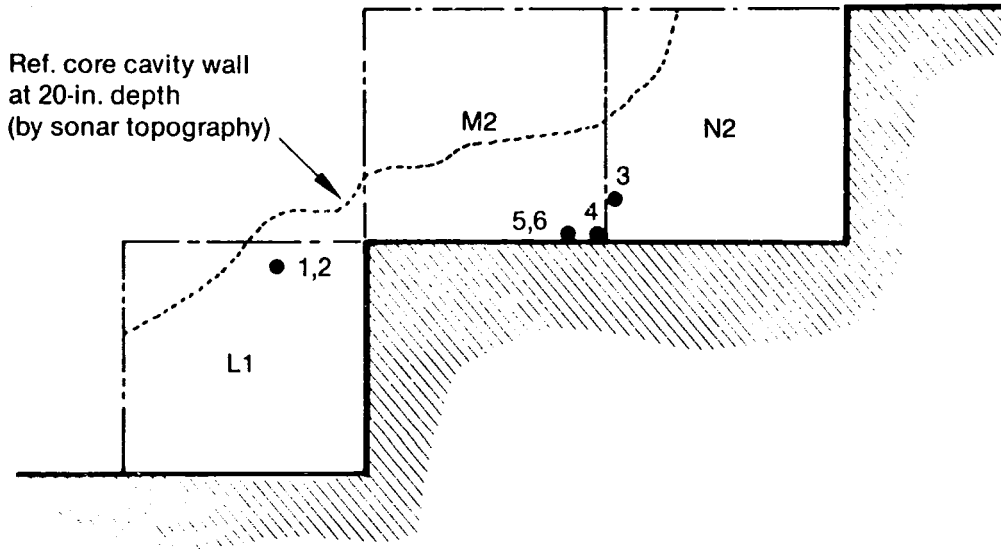
Therefore, causes other than exposure to the short-term temperature during the accident may have affected the characteristics of the fuel rods. They include leaching of core materials and fission products from exposed surfaces and oxidation of surfaces caused by chemical interaction with the coolant.

### 2.3 Segment Locations in the Core

Acquisition information furnished by GPU Nuclear was used to identify the original locations of the fuel rod segments in the core. All of the segments were obtained from sections of fuel rod located between the first and second spacer grids. This corresponds to the area between contour lines 16 and 40 shown in Figure 3.

Figure 4 shows the original locations of the standing fuel rod segments examined. It presents the following information for each segment:

- The segment identification number



Segment	Core Position	Rod Position	Fuel Assembly Axial Region <sup>a</sup>	Extremity Condition	
				Upper	Lower
1	L1	B10	Between upper spacer grids	Sheared	Transition <sup>b</sup>
2	L1	B10	Adjoining (above) Segment 1	Sheared	Sheared
3	N2	N1	Between upper spacer grids	Sheared	Sheared
4	M2	R15	Between upper spacer grids	Sheared	Sheared
5	M2	R13	Between upper spacer grids	Sheared	Sheared
6	M2	R13	Adjoining (below) Segment 5	Sheared	Sheared

a. All segments were obtained from between the first and second spacer grids (52 to 105 cm from the top of the fuel assemblies).

b. A transition region is defined as the interface between the standing fuel rod and prior molten material.

6 10 697

Figure 4. Locations of the standing fuel rod segments retrieved from the TMI-2 core.

- The location (core and rod positions) of the specific standing fuel rod from which each segment was obtained and the fuel assembly axial region
- The condition of the fuel rod segment extremities. Note that only one segment had a possible transition region at one of its extremities.

Figures 5, 6, and 7 are still-images obtained from video survey/monitor recordings (CCTV) of fuel assemblies at core positions L1, N2, and M2. The video surveys were conducted on December 6 and 21, 1985. The video monitoring was conducted during acquisition of the fuel rod segments on December 22, 1985. The December 6 and 21 still-images were made using special video enhancement and still-image production equipment. The December 22 still-images are photographs of the video display monitor. The combination of dark objects, underwater lighting, water turbidity, and video system distortion of the true image caused the image deterioration.

The condition of the fuel assembly at core position L1 is shown in Figure 5. The upper end fitting and fuel rod bundle are only partially intact, with several fuel rods and guide tubes in the northwest quadrant missing. Between the upper end fitting and the next spacer grid, there are zones of interaction between the following:

- Pellet stack holddown spring and fuel rod cladding
- Fuel pellet and fuel rod cladding
- Fuel rods and spacer grids.

Segments 1 and 2 were obtained from fuel rod position B10 (rod location in fuel assembly) of core position L1, which is immediately behind the sixth fuel rod from the left side of the fuel bundle. This section of the fuel rod was divided into two segments; Segment 1 is the lower end with a transition region, and Segment 2 is the adjoining upper segment.

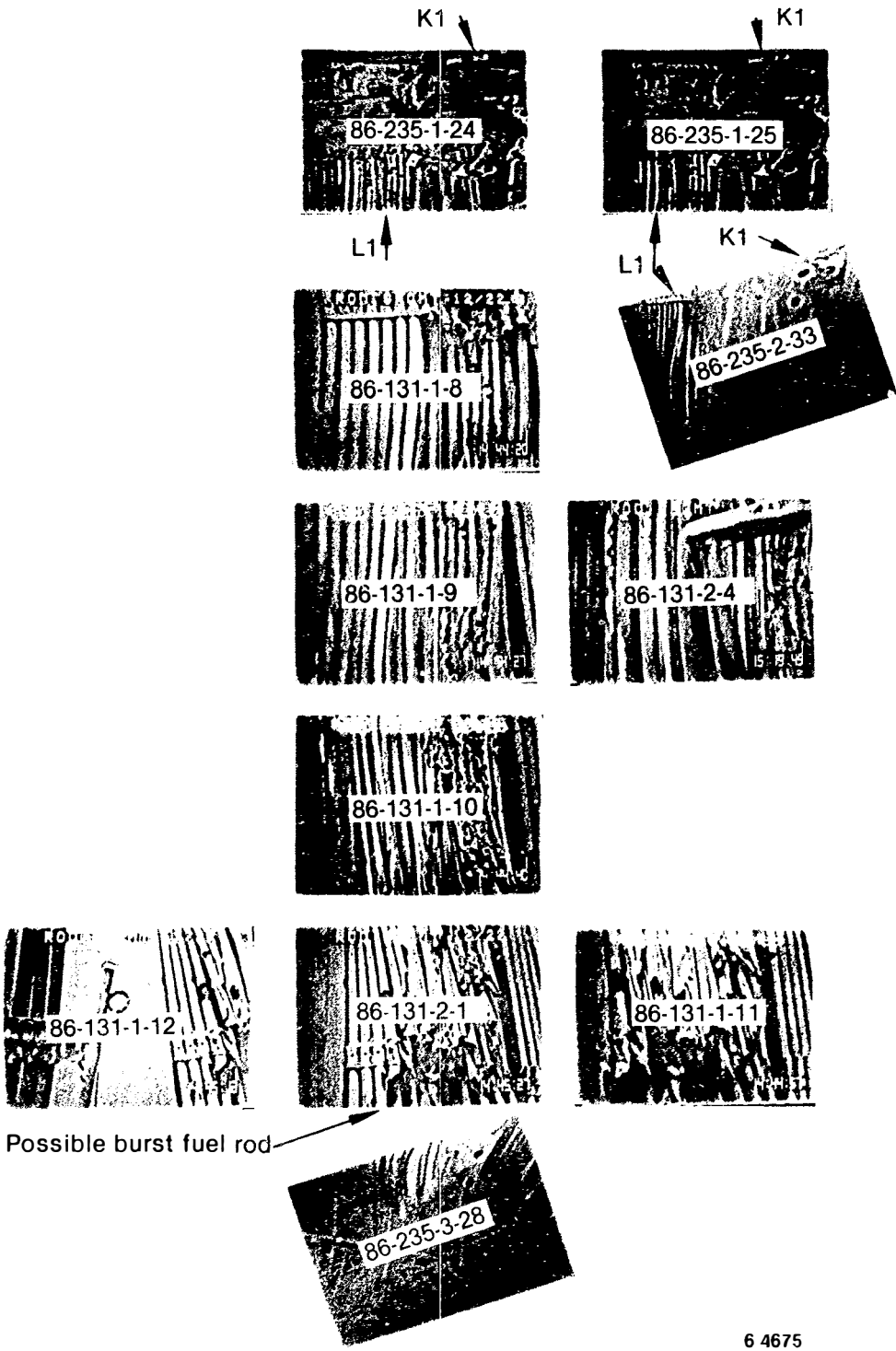
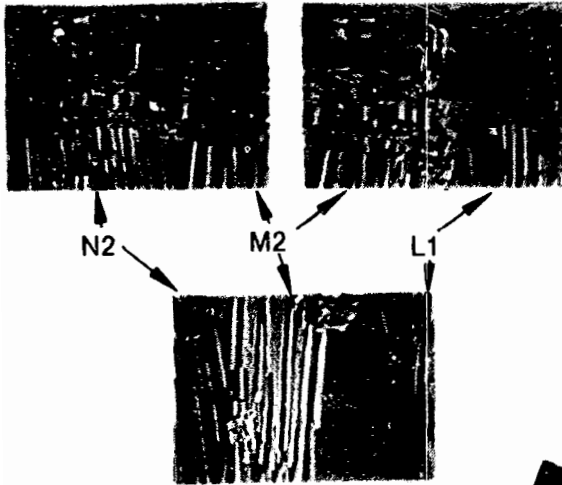
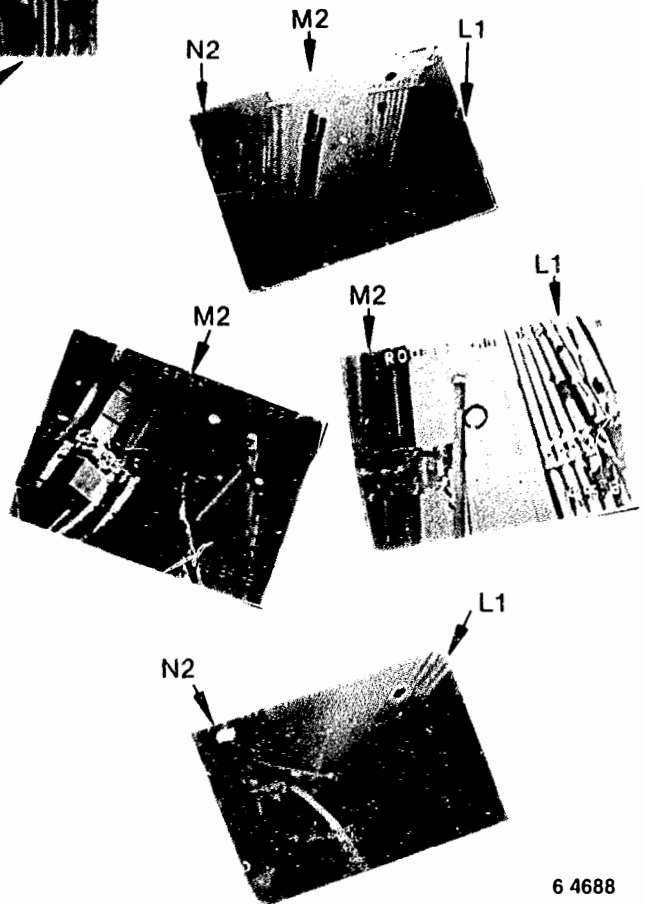


Figure 5. View of the side of the IMI-2 core cavity, showing the fuel assembly at core position L1.

December 6, 1985



December 22, 1985

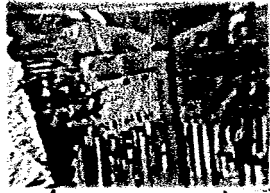


6 4688

Figure 6. View of the side of the TMI-2 core cavity, showing the fuel assembly at core position N2.



12/6/85



12/6/85



O3

N2

M2



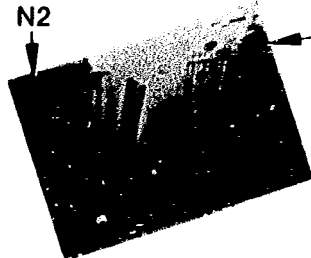
O3

N2

N2

L1

12/16/85



12/16/85

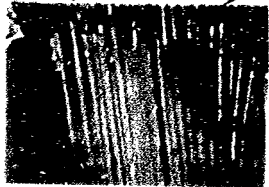
O3

N2

M2

L1

12/6/85



12/6/85

N2

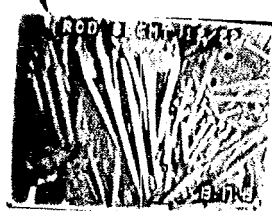
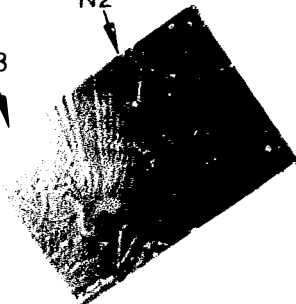
L1

N2

L1

12/16/85

O3



12/16/85

6 4689

Figure 7. View of the side of the TMI-2 core cavity, showing the fuel assembly at core position M2.

The condition of the fuel assembly at core position N2 is shown in Figure 6. The northwest corner of the upper end fitting is ablated, and the fuel rod bundle is partially intact, with more than half of the fuel rods and guide tubes missing in the region where the fuel rod segment was cut.

Segment 3 was cut in the top region of the pellet stack from the position N1 fuel rod of the core position N2 fuel assembly. It appears that the adjacent fuel rod toward the core center is missing, which indicates the fuel rod was close to, or at the perimeter of, the core cavity.

The condition of the fuel assembly at core position M2 is shown in Figure 7. The M2 fuel assembly fell onto the floor of the core cavity sometime between December 6 and 16, 1985, leaving three bent fuel rods still remaining. The remnant of the next spacer grid below the upper end fitting can be seen supporting the three fuel rods. It is believed that the spacer grid remnant is the southeast corner of the spacer grid. It is believed also that the three standing fuel rods are in rod positions R13, R14, and R15, which were adjacent to the core former wall, with R15 also adjacent to a fuel rod from the core position N2 fuel assembly. The core position M2 fuel assembly is badly damaged, with up to half of the upper end fitting tie-plate ablated, and more than half of the fuel rods and guide tubes missing on the north side.

Information obtained from the acquisition of the M2 fuel rod segments and the video monitor recordings indicate the following:

- All three rods from the core position M2 fuel assembly were shortened by amputating the upper extremities with shears near the top of the fuel pellet stack.
- Segment 4 was cut from the top of the shortened, position R15 fuel rod.

- Segments 5 and 6 were cut in sequence from the top of the shortened, position R13 fuel rod.

## 2.4 Segment Acquisition, Packaging, and Shipping

### 2.4.1 Retrieval from the Core

The six fuel rod segments were cut from the standing fuel assembly remnants on December 22, 1985, using a remotely operated vise grip and heavy duty shears. Each segment was approximately 15-cm long. A vise grip was used to firmly hold the fuel rods during shearing and to transfer the segments to nearby (in the core cavity) three-chambered shipping receptacles (fuel pin sample cells). CCTV monitoring of the process was recorded almost continuously and was used as the principal technique for identifying the original location of each segment.

### 2.4.2 Packaging and Shipping

The six fuel rod segments were packaged in concentric vessels for shipment to INEL, identified as follows:

1. An innermost, stainless steel, three-chambered fuel pin sample cell (three segments per sample cell)
2. A specially designed, lead-shielded container
3. A sealed, steel, 10.75-in.-OD by 14.25-in.-long 2R container
4. A general purpose shipping cask designated as the CNSI 1-13 C II cask, manufactured by Chem Nuclear Systems, Inc.

The fuel pin sample cells and shielded container are self-draining, so the fuel rod segments were exposed to air continuously after the sample cell and shielded container were lifted from the water-filled core cavity.

Packing was not used between the segments and the walls of the sample cells. The sample cells and shielded container fit closely together. The shielded container and 2R container also fit together closely. The configuration of the shipping cask after loading consisted of (a) a stack of three 2R containers (two contained the six segments; one was empty) separated by wood pallets and (b) a wood shoring cage to immobilize the 2R containers inside the shipping cask. The cask was transported to INEL by truck. It is assumed that nothing occurred during shearing, packaging, and shipping of the segments to alter their physical condition. There were no identifiably fresh scoring or marks on the rods except at the cutting locations.

### 3. EXAMINATION PLAN AND ANALYTICAL METHODS

Because GPU Nuclear was successful in identifying the specific core positions and fuel rods from which the segments had been obtained, a limited, nondestructive examination plan was developed to characterize the fuel rod segments and determine if they merited further destructive examination. The examination plan was based on using three relatively inexpensive examination techniques available at INEL. The techniques, in order of use, were neutron radiography, gamma spectroscopy, and visual and photographic examinations of the inner and outer surfaces of the segments. The neutron radiography and gamma spectroscopy analyses were performed initially to (a) determine if important features of the rod segments might be disturbed during future cutting operations and (b) locate the pellet interfaces so the segments could be cut at locations that would minimize contamination of the hot cell. The examination methods and procedures are listed below.

- Neutron Radiography--Neutron radiography of the fuel rod segments was performed in the neutron radiography facility of the Coupled Fast Reactivity Measurement Facility at INEL. Two series of measurements were performed, the first after a 45-min irradiation period and the second after a 1-h irradiation to improve resolution of the radiographs.
- Gamma Spectroscopy--The gamma spectroscopy data acquisition system used was a Davidson Model No. 2056-4k, and the detector system was a collimated portable Ortec Hyperpure germanium detector (Model No. GEM-08180-S). Data analysis was done using the gamma spectroscopy analysis code GAP<sup>6</sup> on the Vax computer at the Radiation Measurements Laboratory of INEL.
- Visual and Photographic Examinations--Visual and photographic examinations were performed of (a) the intact segments in plastic storage containers, (b) the segments compared with an intact

piece of fuel rod cladding to evaluate rod deformation, and  
(c) cut surfaces removed to evaluate deformation and oxidation of  
the interior and exterior surfaces of the fuel rod cladding.

## 4. EXAMINATION RESULTS

Results from the neutron radiography, gamma spectroscopy, and visual and photographic examinations of the six fuel rod segments are presented in this section.

### 4.1 Neutron Radiography

Neutron radiography was performed on each of the six fuel rod segments. Radiographs were obtained at two rod orientations (0 and 180 degrees) to evaluate variations in surface characteristics. However, no significant differences were observed between the two orientations, and, therefore, only one radiograph of each segment is presented in this report. The six radiographs are shown in Figures 8 through 10.

Figure 8 shows Segments 1 and 2, which were obtained from fuel assembly position L1, rod position B10. Segment 1 contains an apparent transition region (i.e., an intact portion of the rod which had probably extended either partially or wholly into the high temperature region of the core). The flattened region was observed prior to the cutting operations, and suggests that the pellet loss and subsequent crimping of the fuel rod most likely occurred during the accident. The gamma spectroscopy and visual/photographic examinations of Segment 1 provide further evidence of transition conditions. Segment 2 is from the top of the fuel pellet stack and shows no apparent high temperature effects, such as pellet/cladding interaction.

Figure 9 presents the neutron radiographs of segments from two fuel assembly positions. Segment 3 was obtained from the N2 fuel assembly position, at rod position N1. This segment is from the top of the fuel pellet stack and shows both the end of the pellet stack and a zircaloy sleeve-type spacer instead of the expected a  $ZrO_2$  washer. There is no apparent transition region in this segment; however, there is some possible pellet/cladding interaction. Segment 4 was obtained from the position M2 fuel assembly, at rod position R15. This is an intact rod segment with no apparent interaction regions at any location.

Segment 1

Segment 2

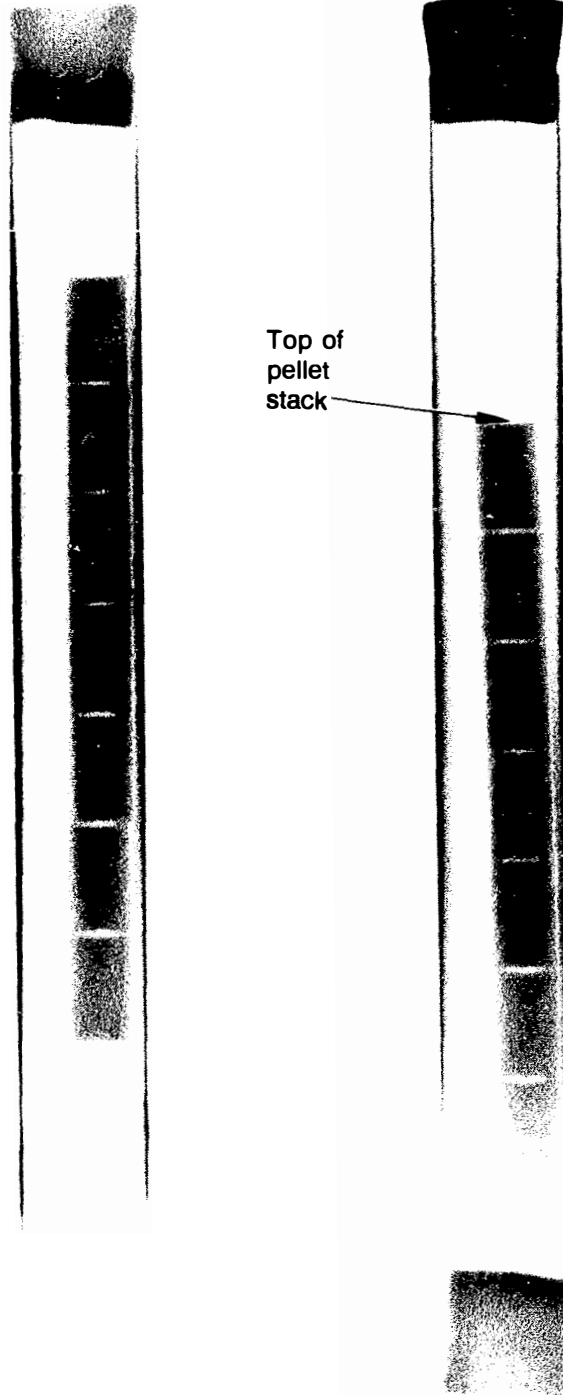


Figure 8. Neutron radiographs of Segment 1 (core position L1, rod position B10, at the transition region) and Segment 2 (core position L1, rod position B10, near the top of the rod).

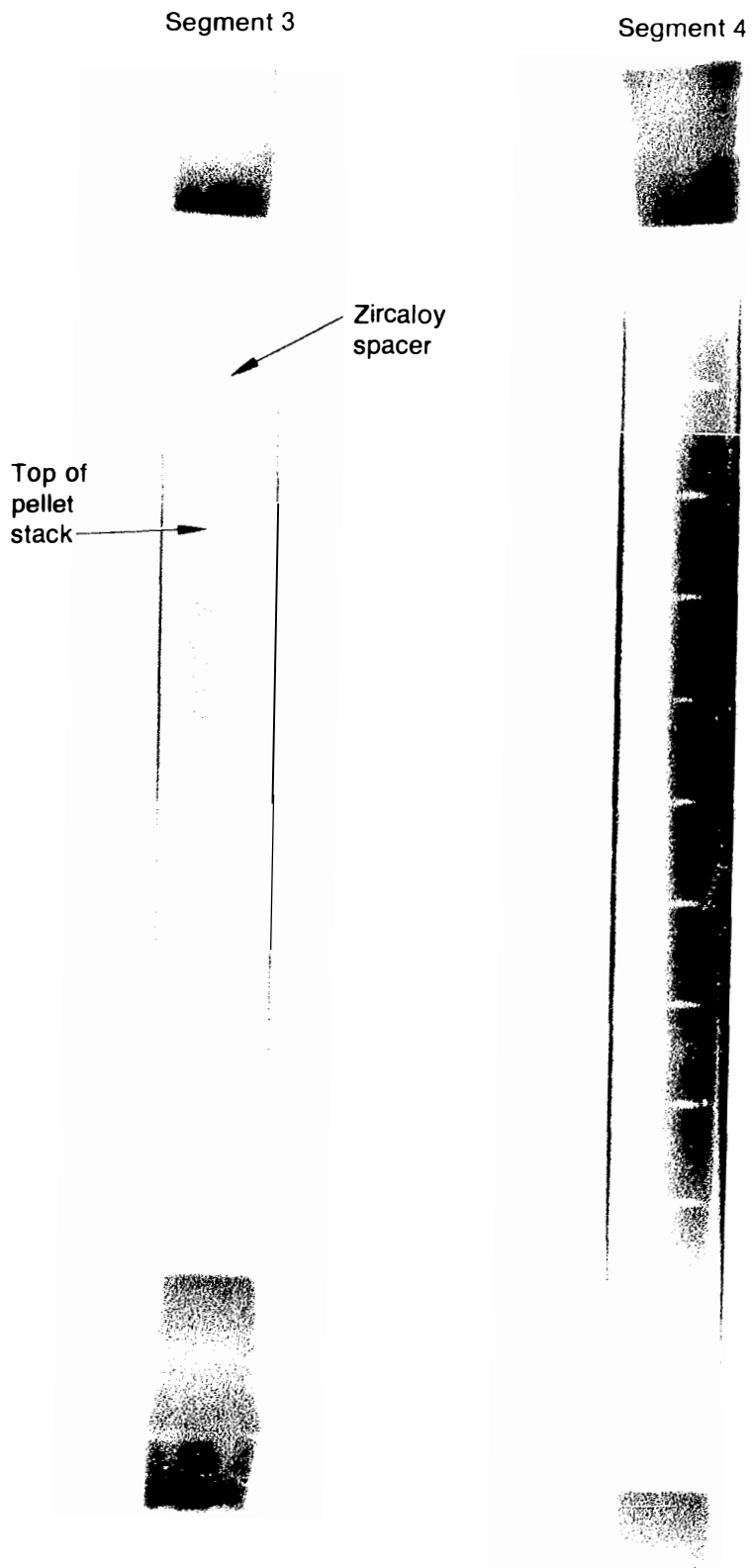


Figure 9. Neutron radiographs of Segment 3 (core position N2, rod position N1) and Segment 4 (core position M2, rod position R15).

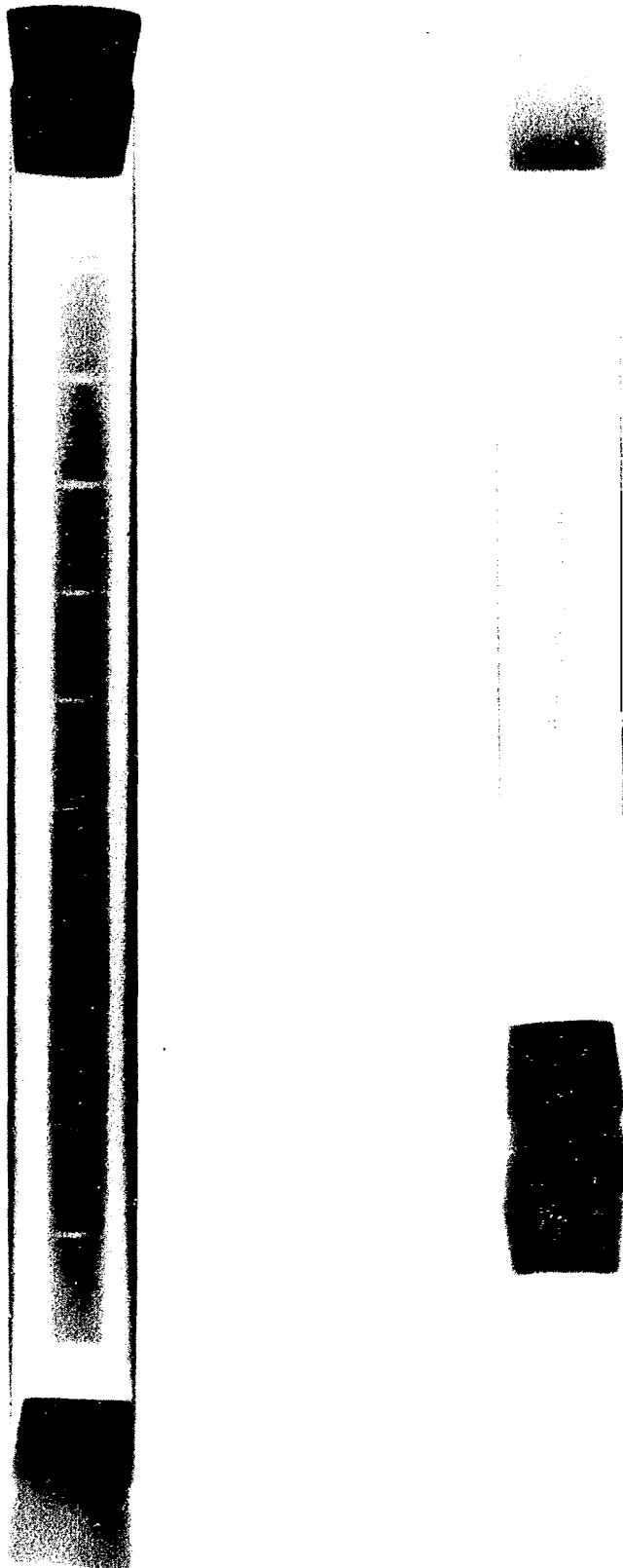


Figure 10. Neutron radiographs of Segment 5 (core position M2, rod position R13, upper segment) and Segment 6 (core position M2, rod position R13, lower segment).

Figure 10 presents the radiographs of two rod segments, also from fuel assembly position M2. Segment 5 is from a location near the top of rod position R13, and Segment 6 was obtained from just below Segment 5. There are no apparent interaction regions or other outstanding features associated with these segments.

Table 2 presents the characteristics of the six fuel rod segments examined, as determined from the neutron radiographs.

#### 4.2 Gamma Spectroscopy

Gamma spectroscopy analyses were performed on the intact fuel rod segments to determine the relative distribution of gamma ray emitters and to compare them with an ORIGEN2 code<sup>7</sup> analysis of the TMI-2 core. A calibration standard was prepared using zircaloy cladding encased lead, with a 5.07-cm-long Eu-152 source placed in a small diameter hole in the center of the simulated fuel rod segment. The calibration measurements and efficiency data are listed in Appendix A. The uncertainty associated with the efficiency data is approximately 50%.

To characterize the fuel rod segments, gamma spectroscopy measurements were obtained at specified lengths along each segment (see Appendix A). The first segment analyzed was Segment 5 (core position M2, rod position R13). Eighteen measurements were taken along the length of this segment, at 1-cm increments. Principal radionuclides measured were Cs-137, Sb-125, Ru-106, Ce-144, Eu-154, and Co-60. Figures 11 through 16 show the distribution of radionuclides along the length of this segment. These data are presented in counts/second at a characteristic gamma ray energy (see Appendix A).

The Cs-137 results shown in Figure 11 indicate a linear reduction in activity from the bottom end (lower in the core) to the top end of the segment. The reduction in activity probably corresponds to the reduction in neutron flux near the outside edges of the core. Variations of this extent are expected near the periphery of the core. The fission products Sb-125, Ru-106, Ce-144, and Eu-154 show corresponding reductions in

TABLE 2. FUEL ROD SEGMENT CHARACTERISTICS<sup>a</sup>

<u>Segment</u>	<u>Core Position</u>	<u>Rod Position</u>	<u>Length (cm)</u>	<u>Number<sup>a</sup> of Fuel Pellets</u>	<u>Comments</u>
1	L1	B10	17.5	7	Apparent collapse of rod after pellet loss
2	L1	B10	15	8	Spacer
3	N2	N1	10	6.2	Possible pellet cladding interaction near the top and bottom
4	M2	R15	19.5	11.3	No apparent interaction zones
5	M2	R13	18	10.3	Intact rod--no interaction zones
6	M2	R13	10.5	6.5	Intact rod--no interaction zones

a. Determined from neutron radiographs.

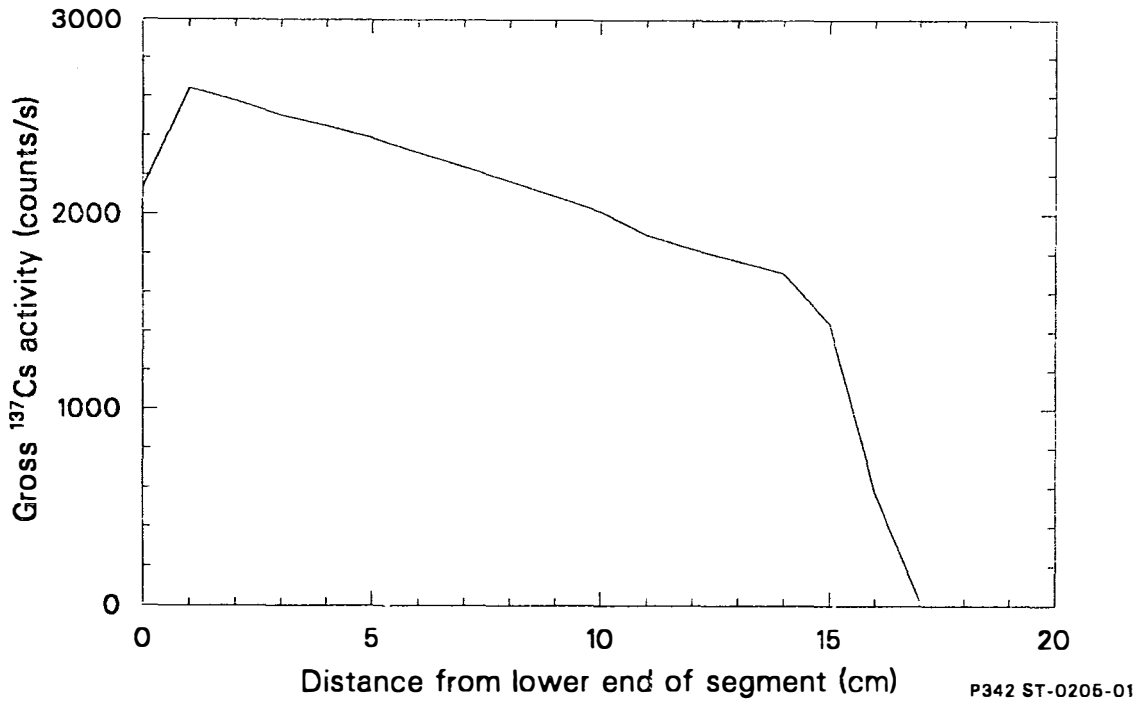


Figure 11. Gross Cs-137 distribution along Segment 5.

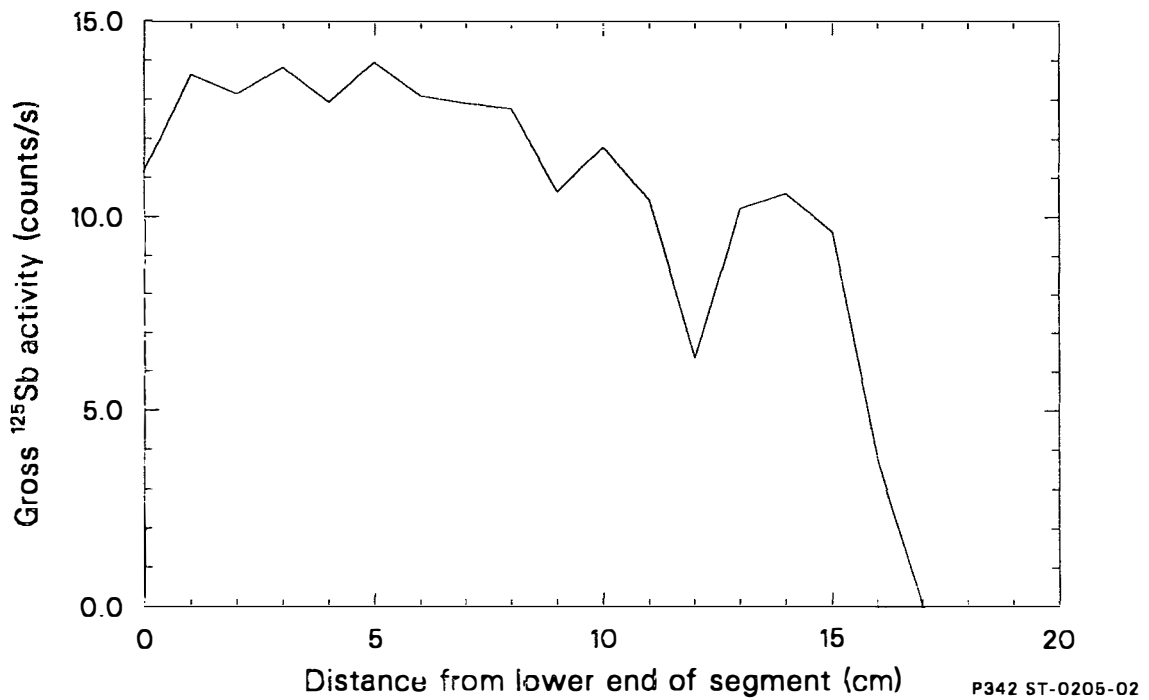


Figure 12. Gross Sb-125 distribution along Segment 5.

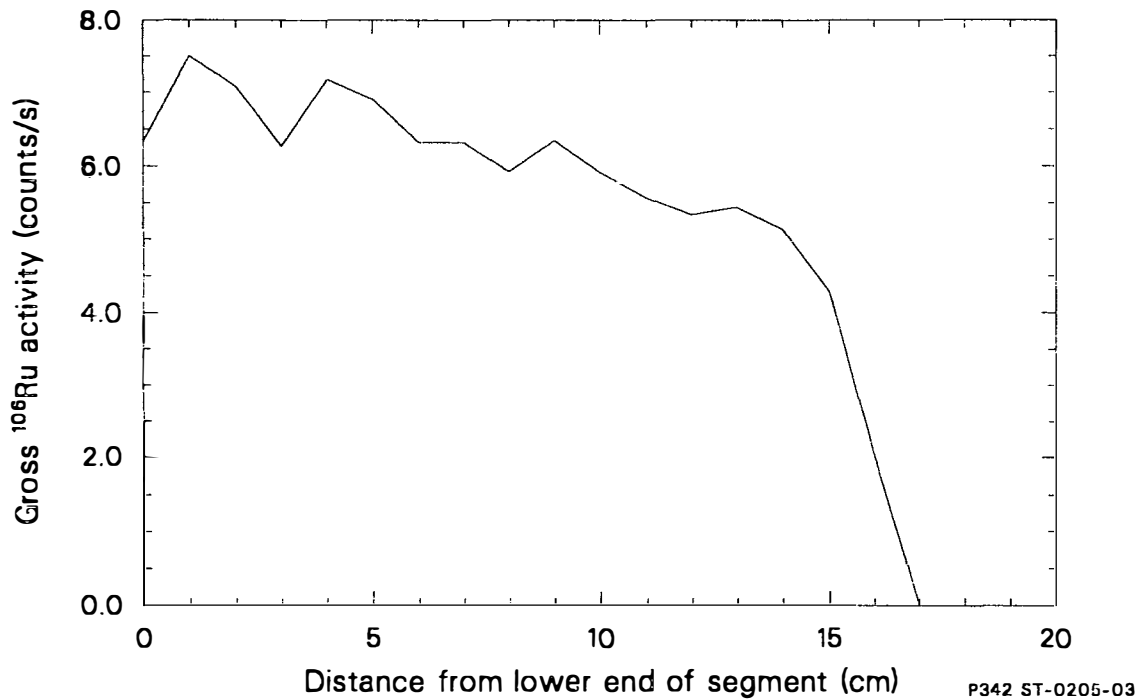


Figure 13. Ru-106 distribution along Segment 5.

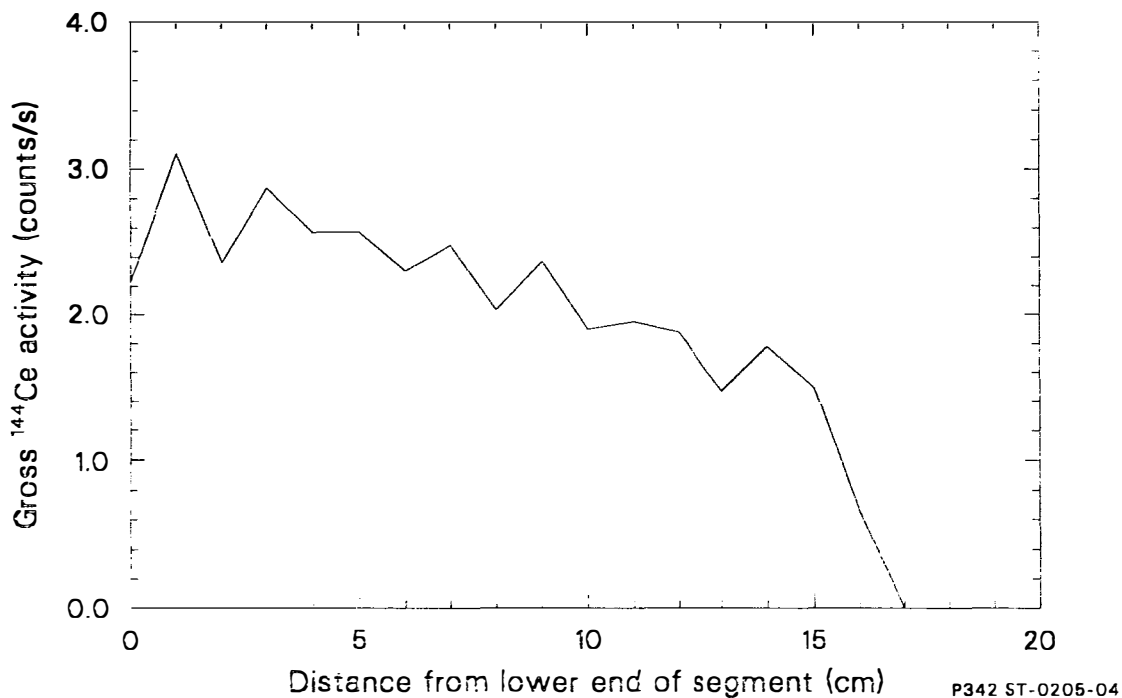


Figure 14. Ce-144 distribution along Segment 5.

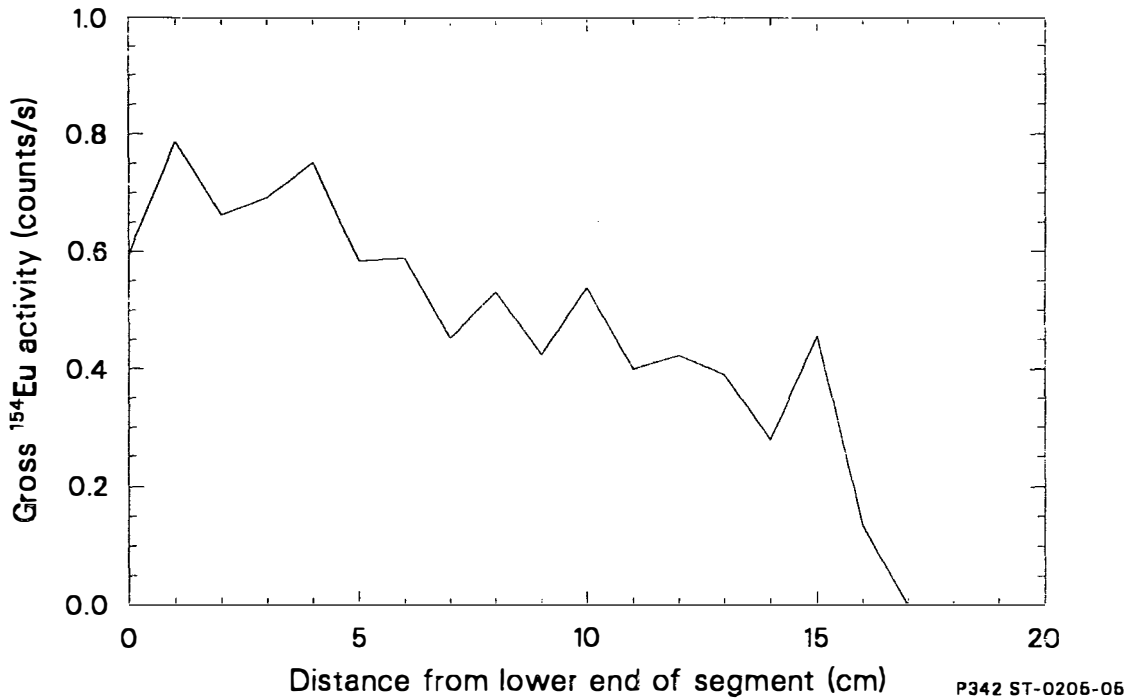


Figure 15. Eu-154 distribution along Segment 5.

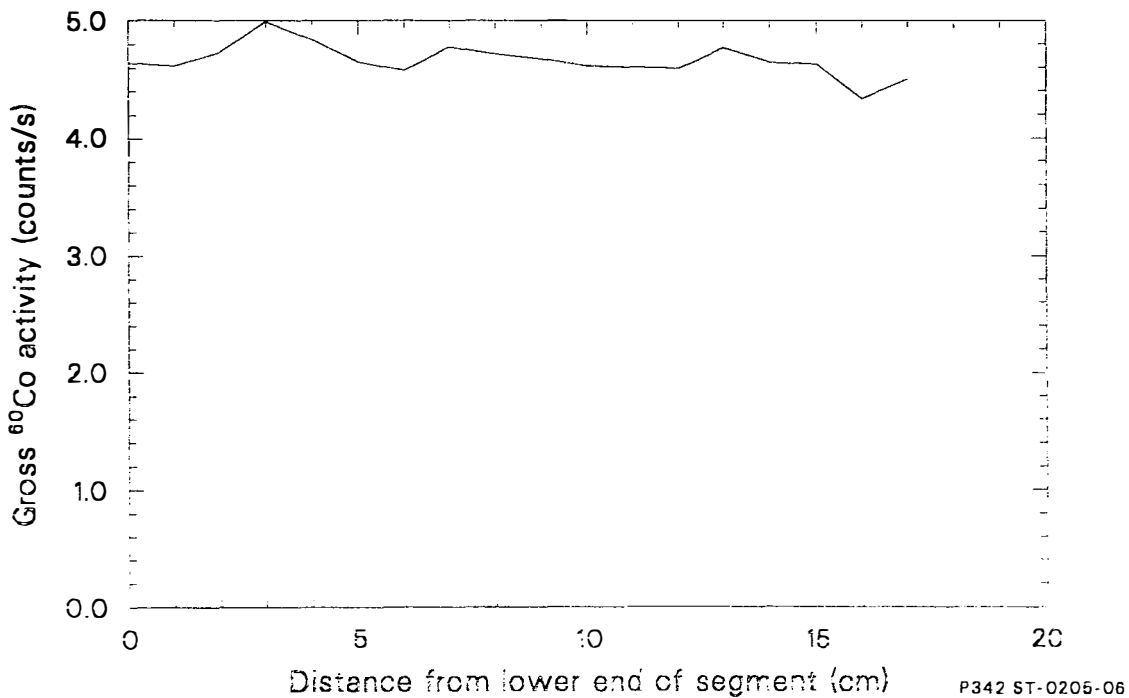


Figure 16. Co-60 distribution along Segment 5.

activity (Figures 12 through 15). The variability in the measured activities is within the uncertainty associated with the measurements. The Co-60 measurements shown in Figure 16 do not indicate the same consistent reduction in activity, probably because of corrosion materials deposited on the surfaces of the segment. The measured count rates (405 cts/sec) suggest relatively low surface concentrations.

After examining Segment 5, which indicated relatively constant activity distributions along the segment for all fission products, the remaining segments were analyzed at the center and each end to define potential activity gradients. These data are listed in Appendix A.

A comparison was performed to determine if the fuel rod segments showed approximately the same concentrations of fission products as predicted by the ORIGEN2 code. This analysis is not precise, as there are some differences in geometry between the calibration standard and the actual rod segments. As previously noted, the uncertainty associated with the efficiency data is on the order of about 50%. A more accurate calibration method (which was beyond the scope of this study) would involve removing samples for radiochemical analysis from an intact fuel rod segment and then calibrating, using the intact segment.

Table 3 lists the ORIGEN2 calculated burnup range for each of the six segment locations. These burnup data were used to generate the average ORIGEN2 calculated radionuclide concentrations (see Reference 7). Table 4 compares the measured and ORIGEN2 calculated concentrations at three segment locations.

The concentrations for all radionuclides except Eu-154 are within approximately 50% of the predicted values (i.e., approximately within the uncertainty of this analysis). The lower-than-expected results may also be attributed to the fact that the elevation of the sampled rod is not accurately known. The Eu-154 concentrations are significantly lower than predicted by ORIGEN2. This is possible because the production of Eu-154 is via a neutron capture process, which makes calculation of expected concentrations very uncertain.

TABLE 3. ORIGEN2 CALCULATED BURNUP RANGES AT SEGMENT LOCATIONS

---

<u>Segment<sup>a</sup></u>	<u>Burnup<sup>b</sup></u> <u>(MWd/MTU)</u>
1	967-2186
2	967-2186
3	911-1806
4	1456-2974
5	1456-2974
6	1456-2974

---

a. The six fuel rod segments all are of the 2.96-wt%-enrichment category.

b. Corresponds to Fuel Group 9 of the ORIGEN2 code (Reference 7). The burnup data are listed as ranges because the sampling locations could not be defined more accurately.

---

TABLE 4. COMPARISON OF MEASURED AND ORIGEN2 CALCULATED RADIONUCLIDE CONCENTRATIONS AT THREE SEGMENT LOCATIONS

Radionuclide <sup>b</sup>	Energy (KeV)	Relative Intensity (gammas/disintegration)	ORIGEN-2 Calculated Concentration (µCi/g)	Segment and Location <sup>a</sup>					
				Segment 5 (Measurement 6)		Segment 3 (Measurement 3)		Segment 6 (Measurement 2)	
				Measured <sup>c</sup> Concentration (µCi/g)	Fractional Retention (%)	Measured <sup>c</sup> Concentration (µCi/g)	Fractional Retention (%)	Measured <sup>c</sup> Concentration (µCi/g)	Fractional Retention (%)
<sup>137</sup> Cs	661.6	85	4.20 E+3	3.6 E+3	86	2.02 E+3	48	4.5 E+3	110
<sup>125</sup> Sb	427.9	31	1.06 E+2	6.35 E+1	60	4.2 E+1	40	7.1 E+1	67
<sup>106</sup> Ru	621.8	11	1.04 E+2	8.14 E+1	78	4.5 E+1	43	1.01 E+2	97
<sup>144</sup> Ce	696.5	1.5	2.21 E+2	2.16 E+2	98	9.8 E+1	44	2.94 E+2	133
<sup>154</sup> Eu	1274	37	1.19 E+1	2.20	18.6	0.58	5.0	4.18	3.5

a. See Appendix A.

b. <sup>60</sup>Co is an activation product of structural materials, so is not included in this table.

c. Measured concentrations calculated by:

$$\frac{\text{counts}}{s} \times \frac{1}{\text{Efficiency}} \times \frac{1}{\text{Relative Intensity}} \times \text{Conversion Factor} \times \frac{1}{\text{Length of Segment Viewed}} \times \text{Conversion to Mass} = \text{Concentration}$$

$$\frac{\text{counts}}{s} \times \frac{\text{gammas}}{\text{count}} \times \frac{\text{disintegrations}}{\text{gamma}} \times \frac{\mu\text{Ci}}{3.7 \times 10^4 \frac{\text{disintegrations}}{s}} \times \frac{1}{1.8 \text{ cm}} \times \frac{1 \text{ cm}}{7.28 \text{ g}} = \frac{\mu\text{Ci}}{\text{g}}$$

Unit Conversion Factors:  $\frac{\mu\text{Ci} - s - \text{cm}}{\text{d} - \text{cm} - \text{g}}$

- <sup>137</sup>Cs = 1.51
- <sup>125</sup>Sb = 4.55
- <sup>106</sup>Ru = 1.18 E+1
- <sup>144</sup>Ce = 8.42 E+1
- <sup>154</sup>Eu = 3.77

### 4.3 Visual and Photographic Examinations

Each fuel rod segment was subjected to both visual and photographic examinations and compared with a portion of new cladding to evaluate deformations (bends or thickness variations) in the cladding. Figures 17 through 34 show side, top, and/or bottom views of each of the rod segments.

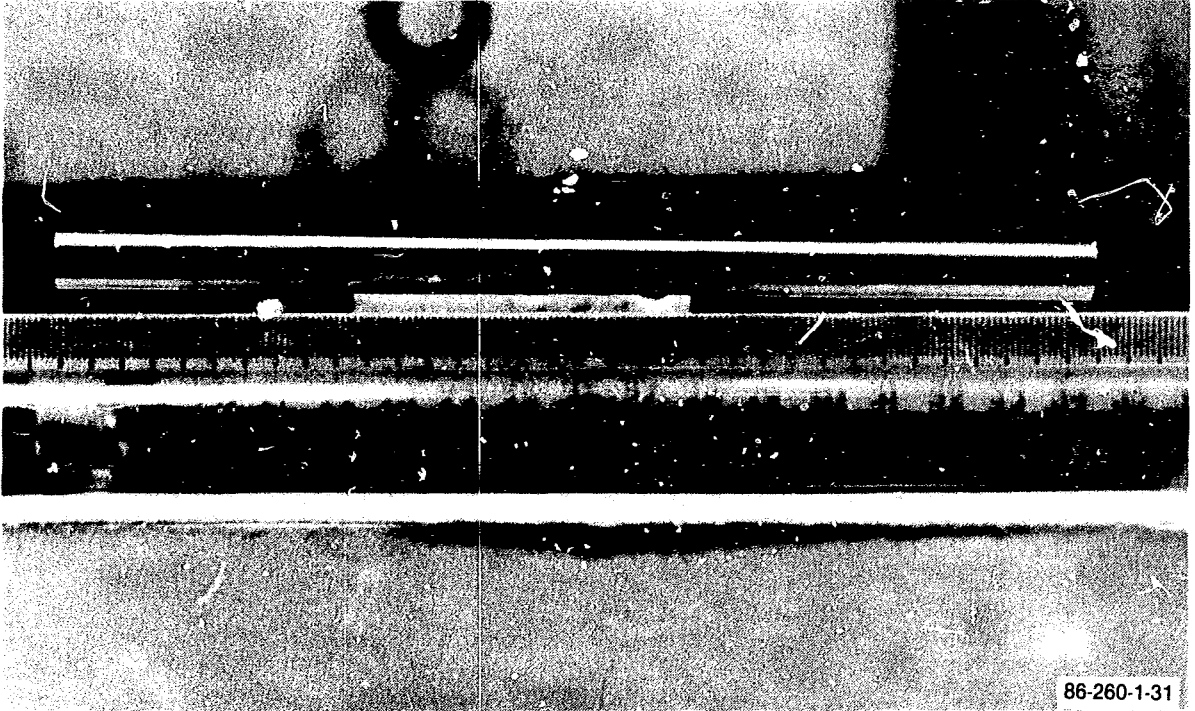


Figure 17. Side view of Segment 1 inside the container tube, showing the transition region at the right end. A new segment of fuel rod cladding is shown above for comparison.

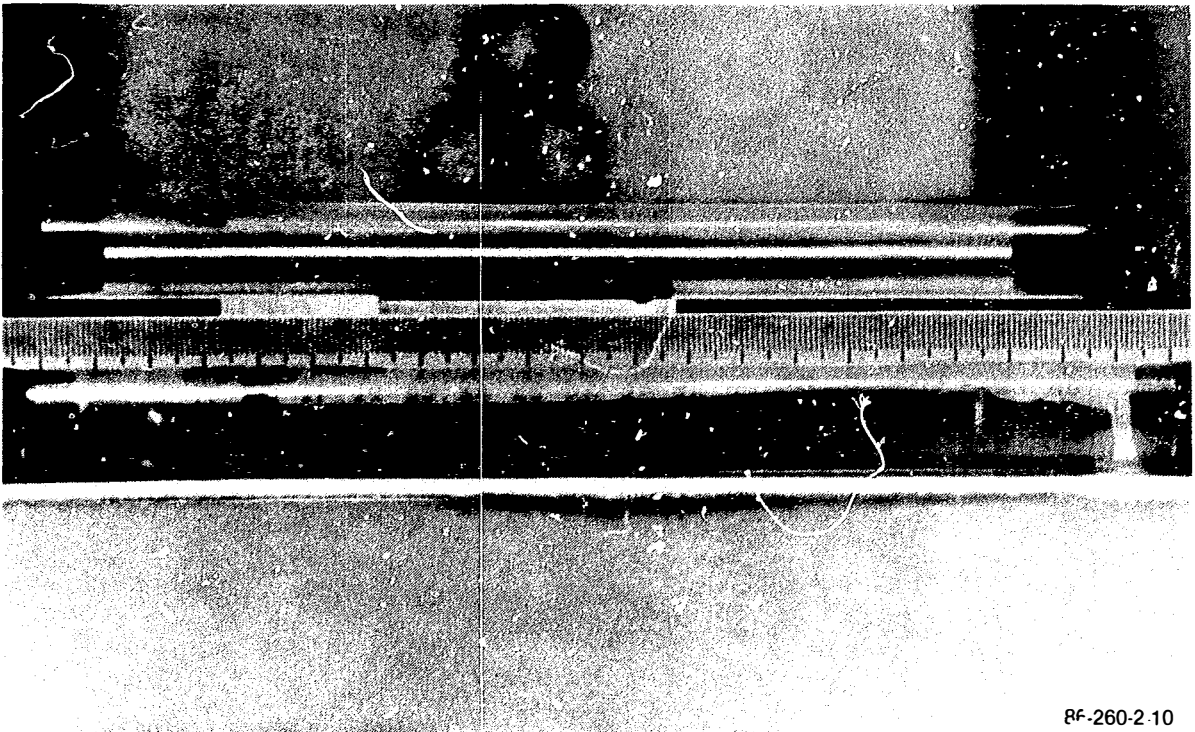


Figure 18. Side view of Segment 1 inside the container tube, showing the transition region at the right end. A new segment of fuel rod cladding inside a container tube is shown above for comparison.

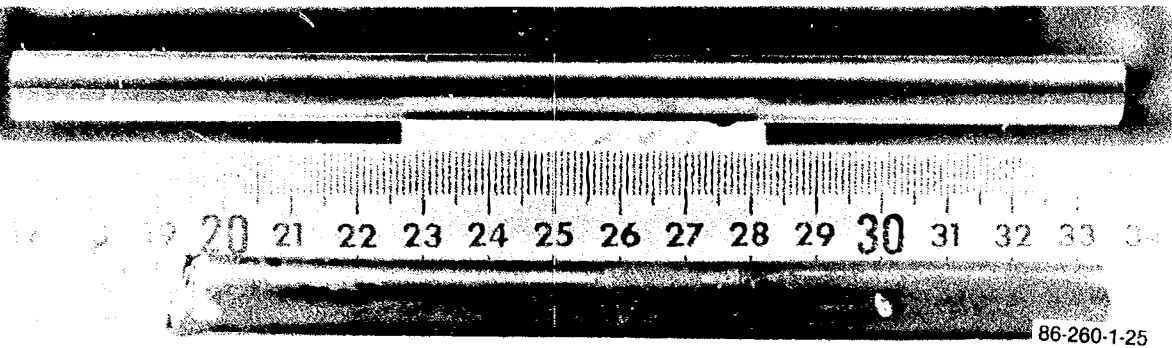


Figure 19. Side view of Segment 2, after sectioning removal of the lower end deformed by the TMI-2 defueling shear tool. A new segment of fuel rod cladding is shown above for comparison.

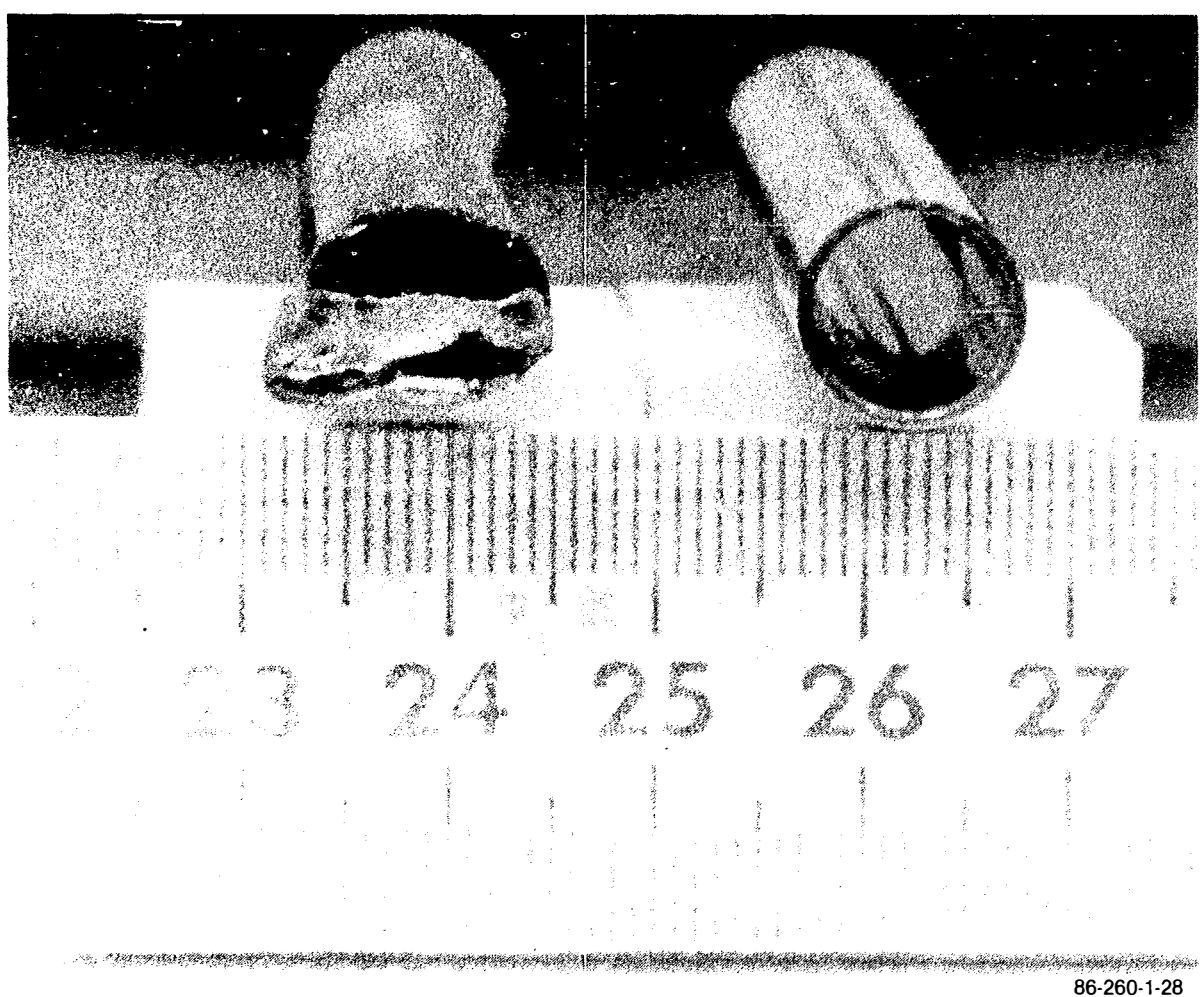
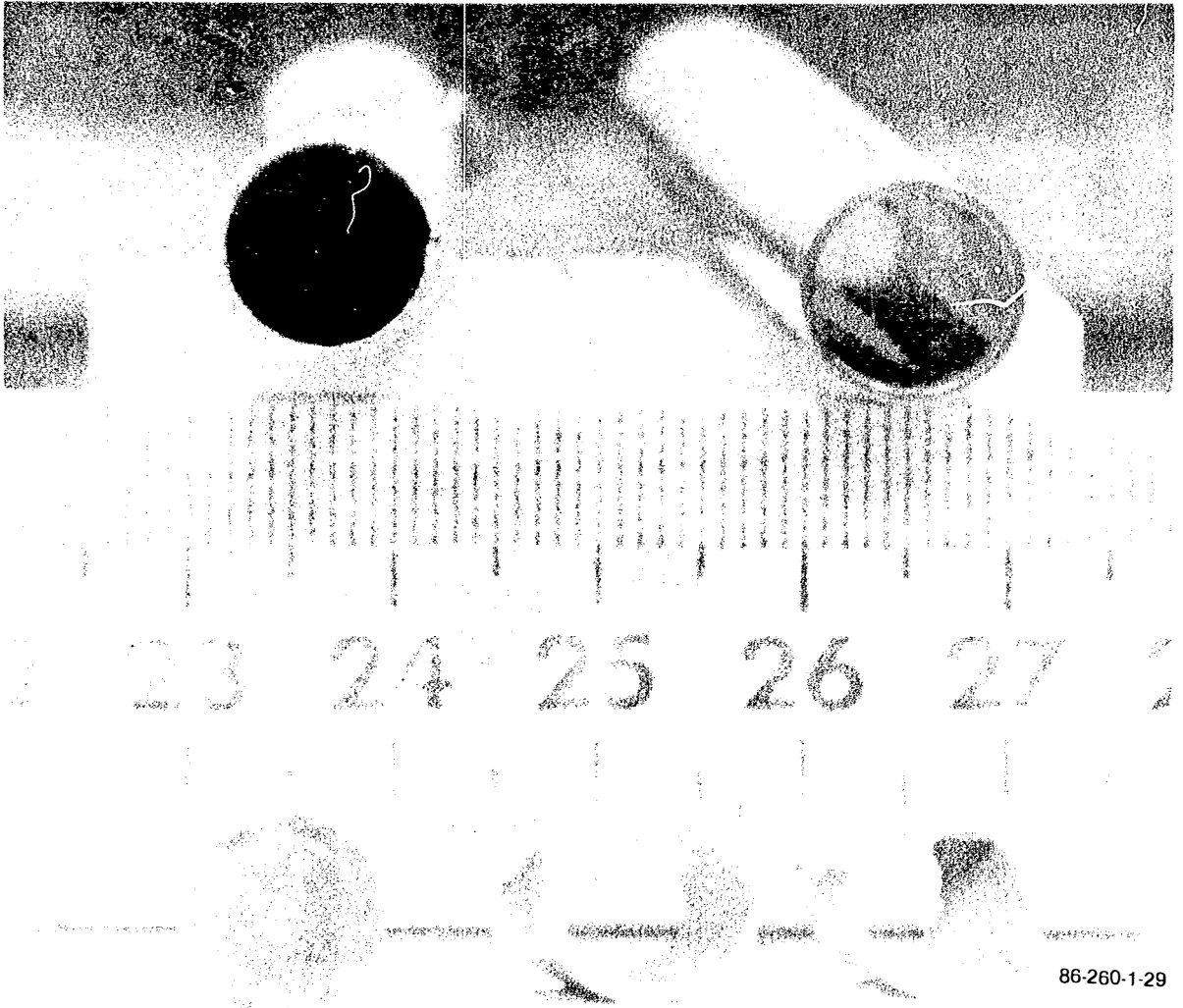


Figure 20. View of Segment 2, showing the top end deformed by the TMI-2 defueling shear tool and the top end of the zircaloy spacer sleeve, which was between the fuel pellet stack hold-down spring and the pellet stack. A new segment of fuel rod cladding is shown at the right for comparison.



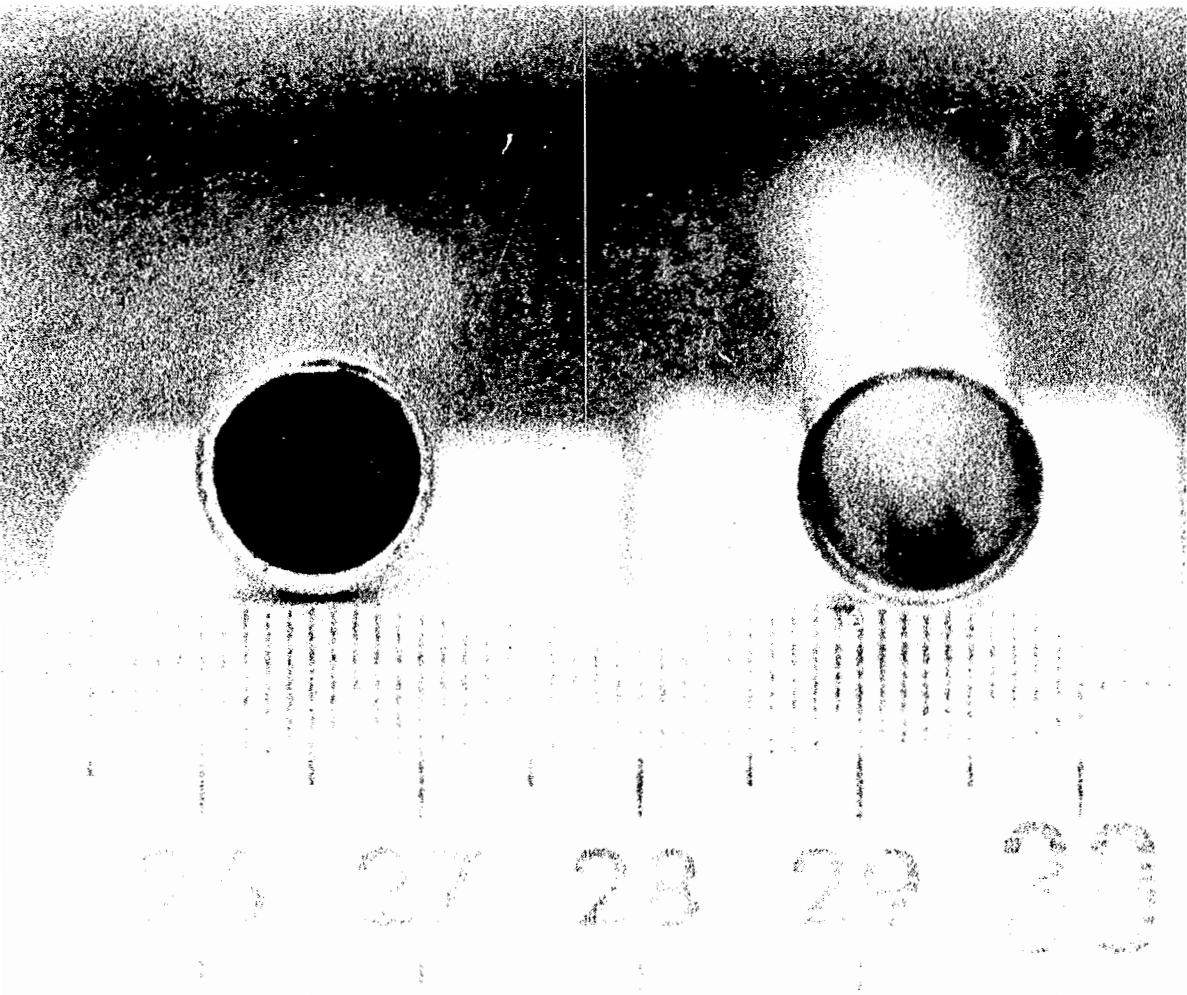
86-260-1-29

Figure 21. Bottom end view of Segment 2, after sectioning removal of both ends deformed by the TMI-2 defueling shear tool. Removed ends are shown below, and a new segment of fuel rod cladding is shown for comparison.

21 22 23 24 25 26 27 28 29 30

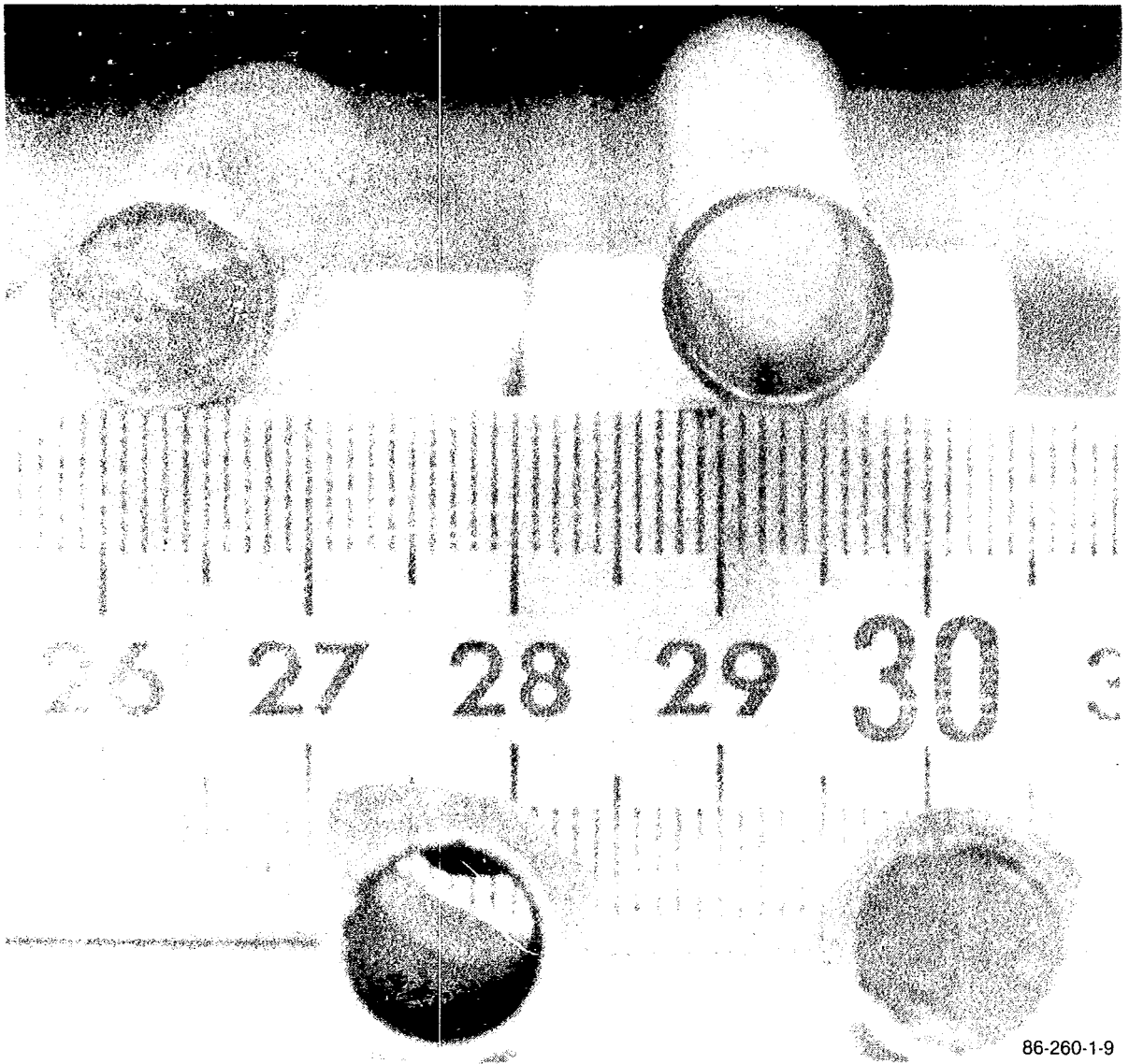
86-260-1-13

Figure 22. Side view of Segment 3, after sectioning removal of both ends deformed by the TMI-2 defueling shear tool. A new segment of fuel rod cladding is shown above for comparison.



86-260-1-6

Figure 23. Top end view of Segment 3, after sectioning removal of the top end deformed by the TMI-2 defueling shear tool. A new segment of fuel rod cladding is shown at the right for comparison.



86-260-1-9

Figure 24. Bottom end view of Segment 3, after sectioning removal of both ends deformed by the TMI-2 defueling shear tool. Removed ends are shown below and a new segment of fuel rod cladding is shown at the right for comparison.

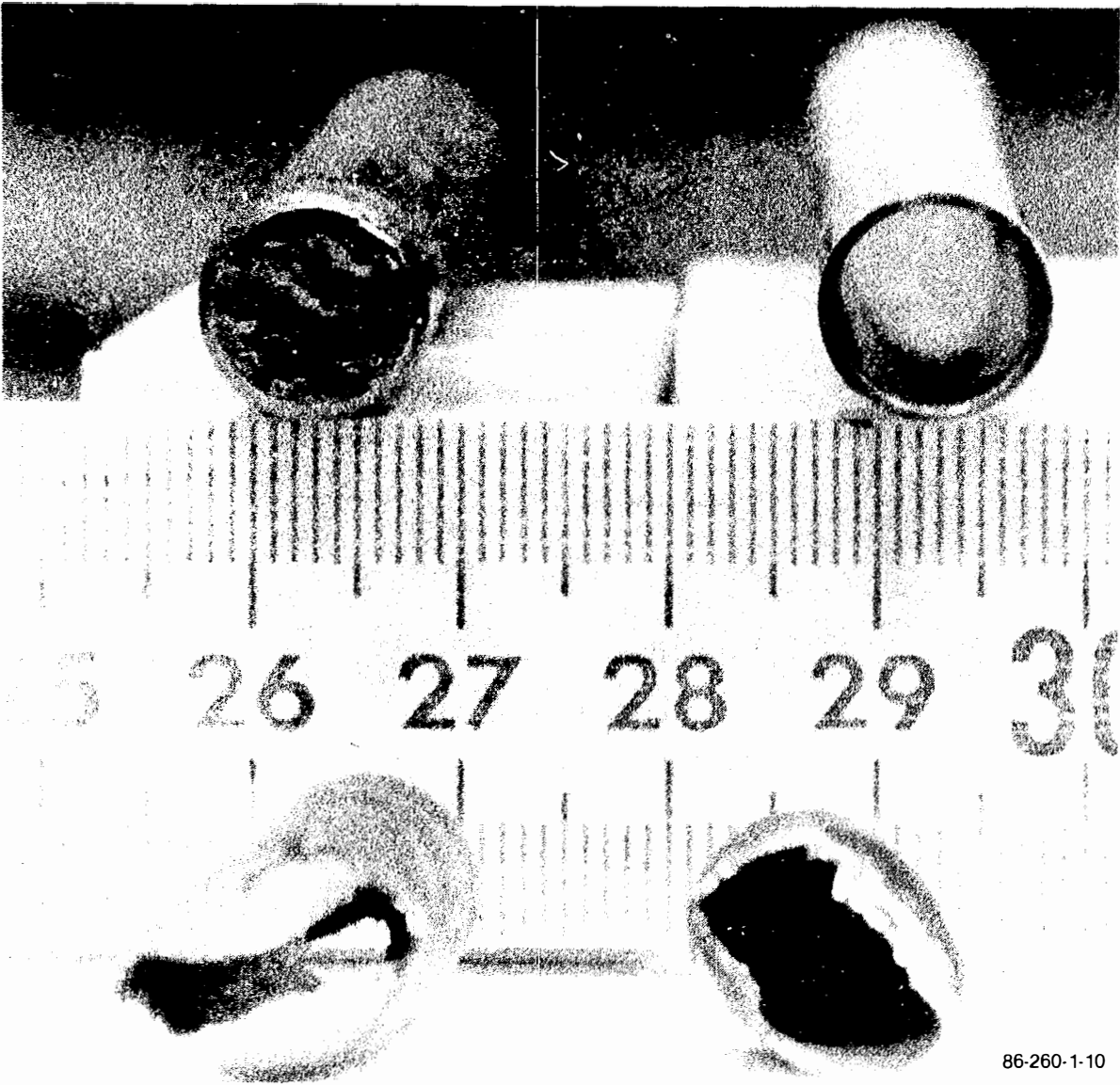
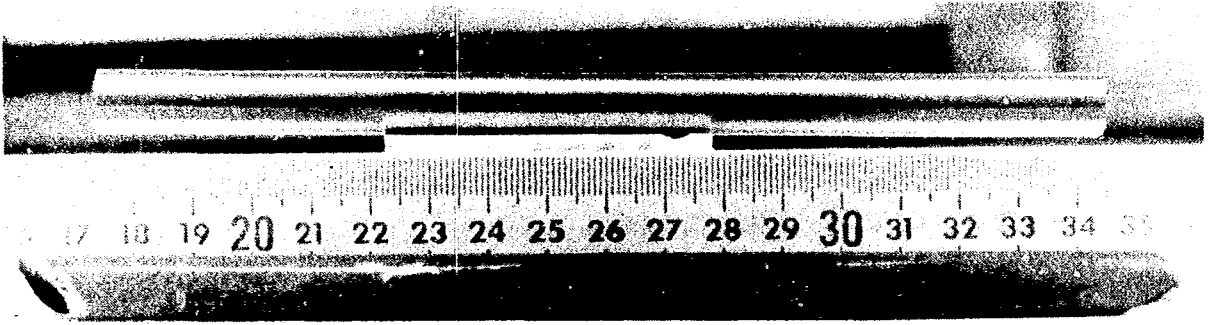
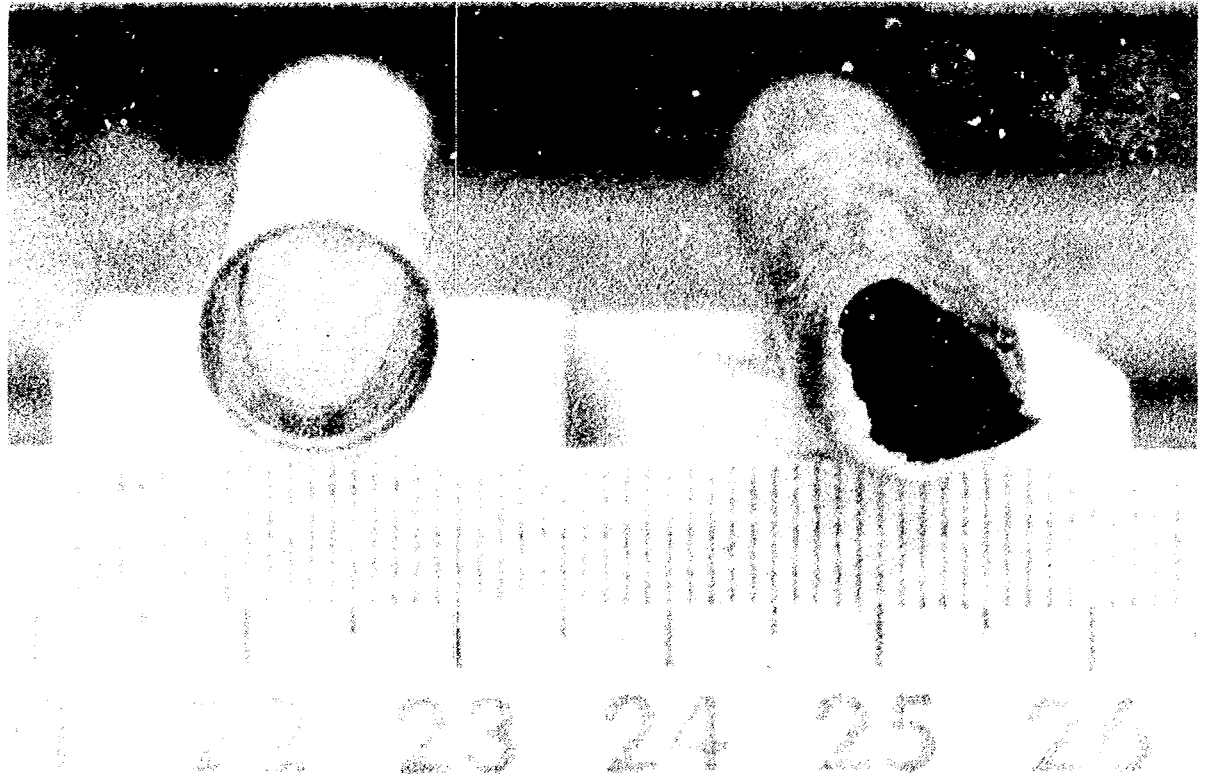


Figure 25. Bottom end view of Segment 3, after sectioning removal of both ends deformed by the TMI-2 defueling shear tool. Removed ends are shown below, and a new segment of fuel rod cladding is shown at the right for comparison.



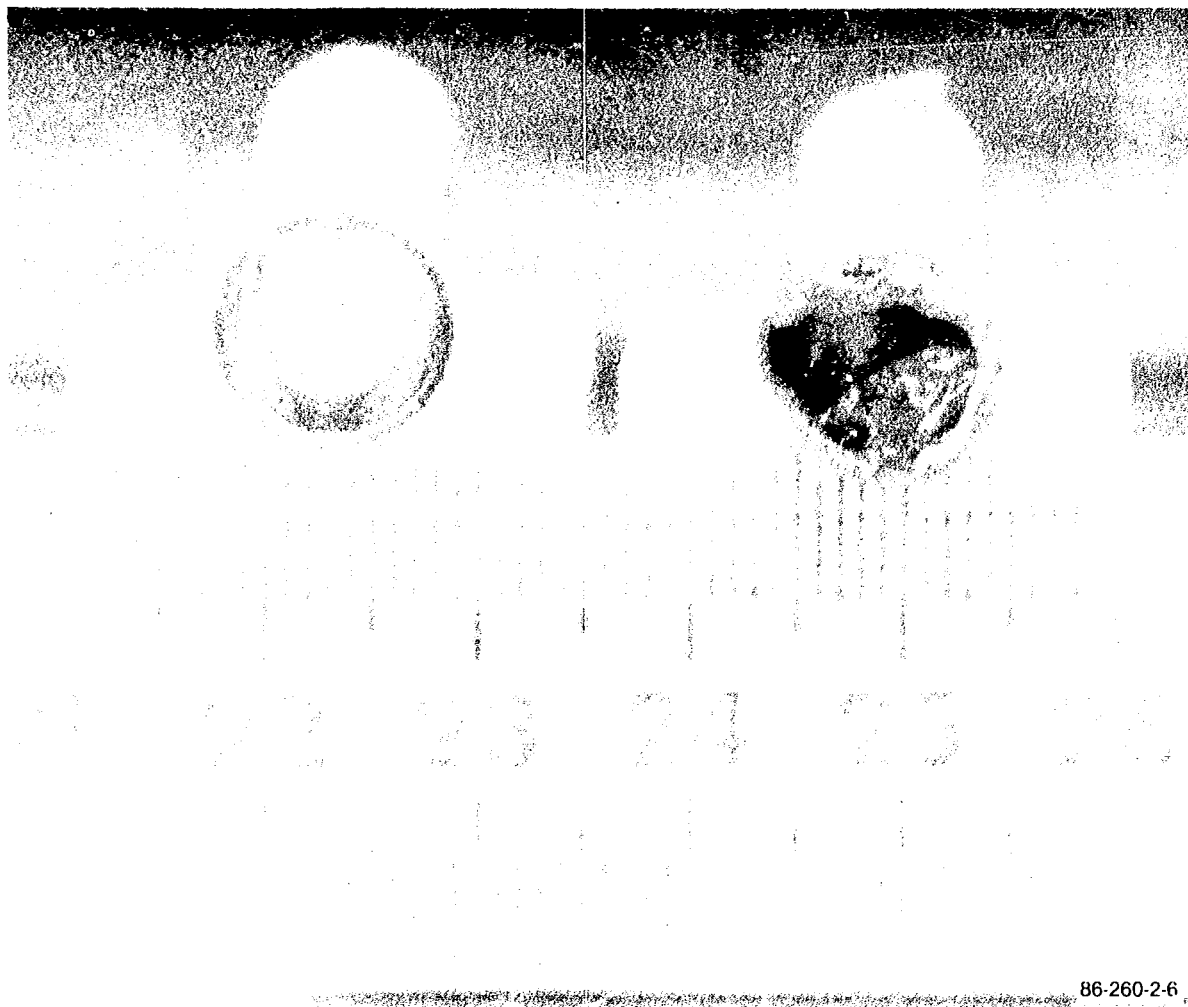
86-260-1-35

Figure 26. Side view of Segment 4, showing both ends deformed by the TMI-2 defueling shear tool. A new segment of fuel rod cladding is shown above for comparison.



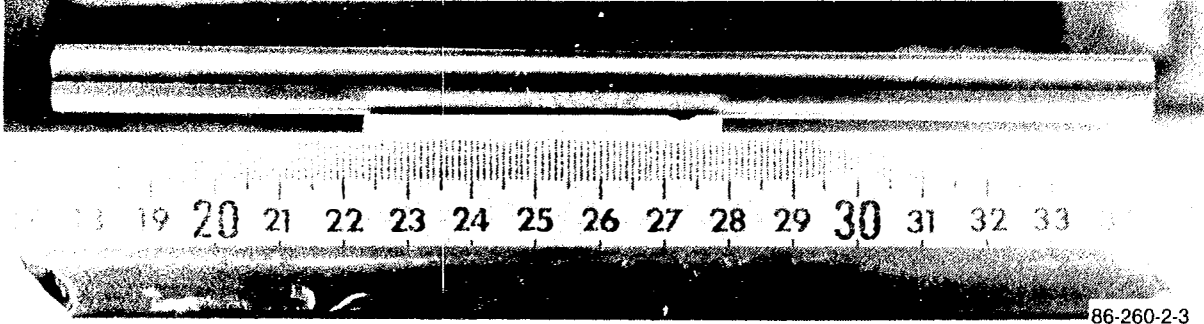
86-260-2-5

Figure 27. View of Segment 4, showing the top end deformed by the TMI-2 defueling shear tool. A new segment of fuel rod cladding is shown at the left for comparison.



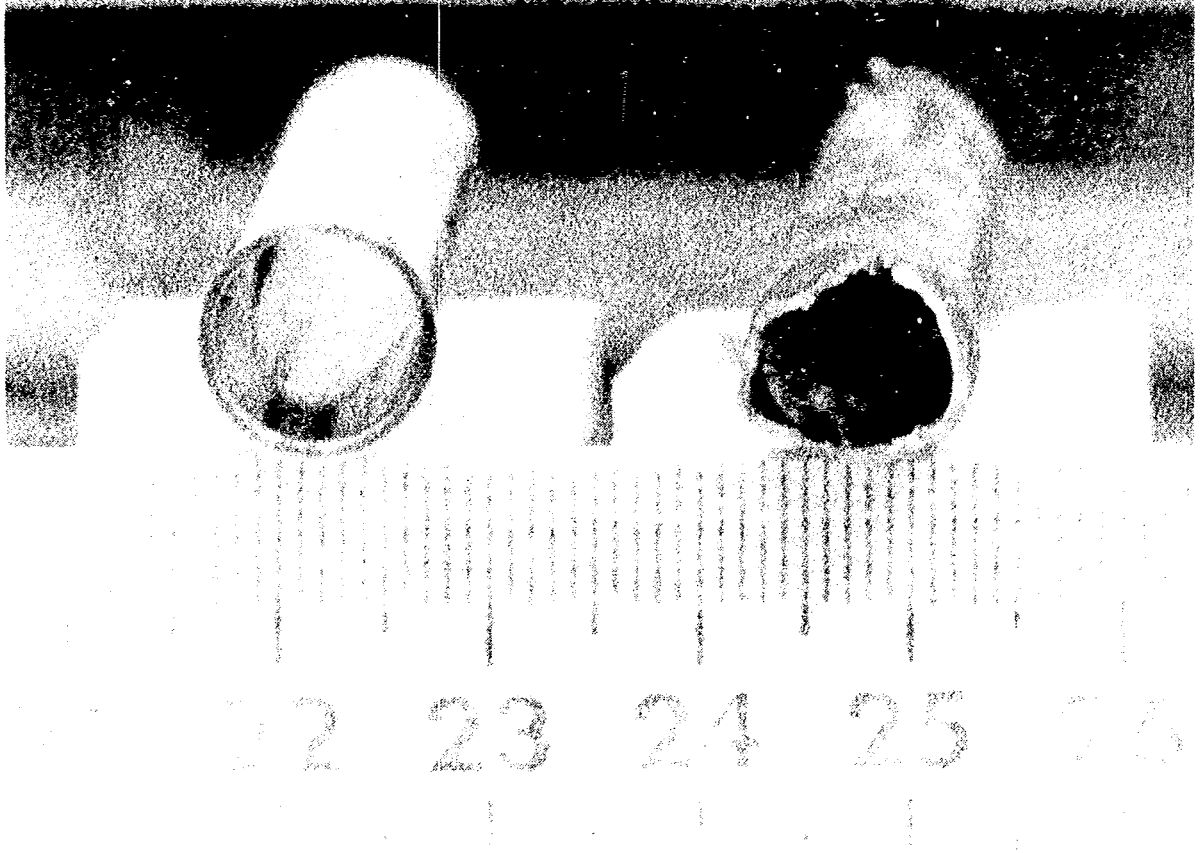
86-260-2-6

Figure 28. View of Segment 4, showing the bottom end deformed by the TMI-2 defueling shear tool. A new segment of fuel rod cladding is shown at the left for comparison.



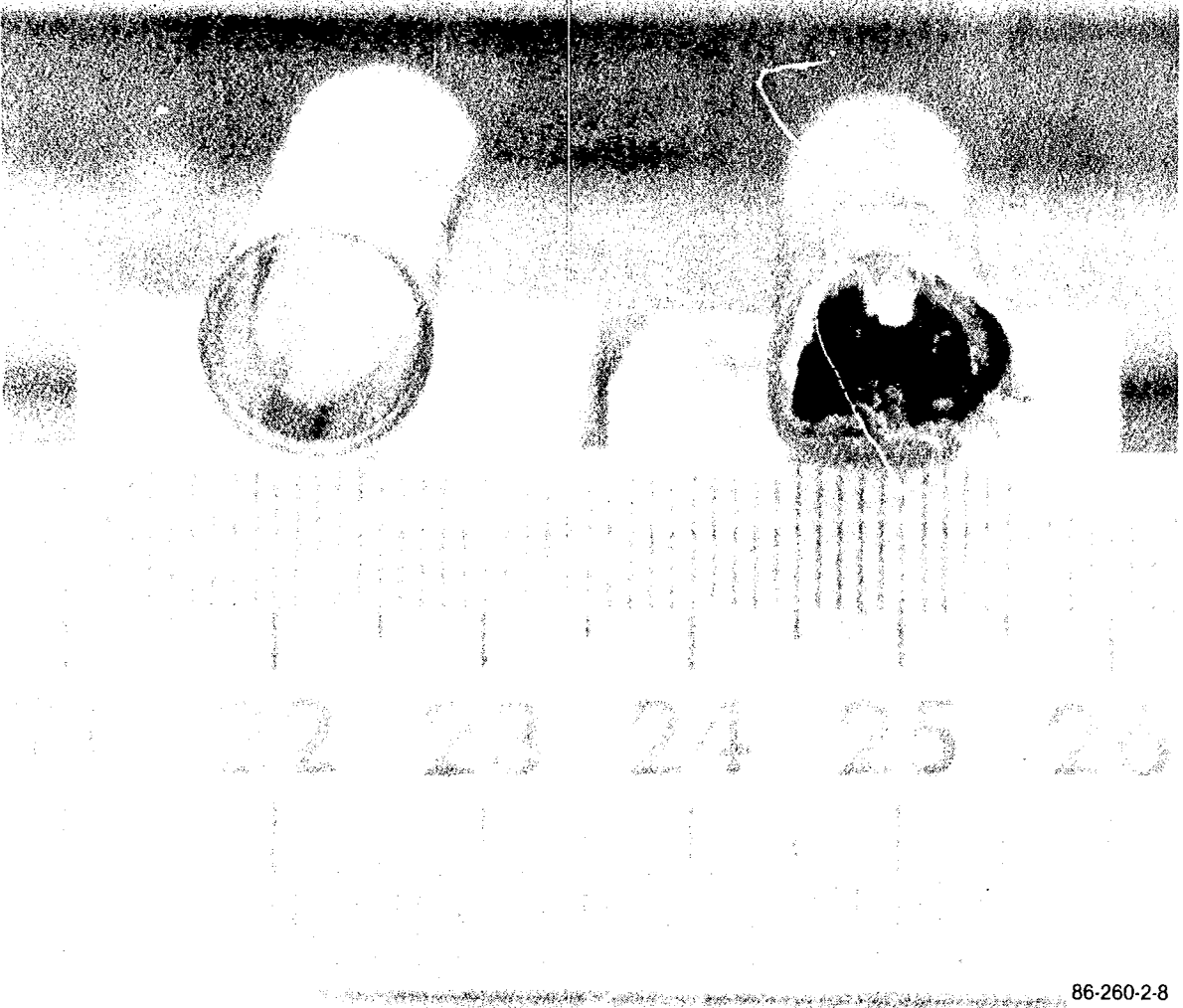
86-260-2-3

Figure 29. Side view of Segment 5, showing both ends deformed by the TMI-2 defueling shear tool. A new segment of fuel rod cladding is shown above for comparison.



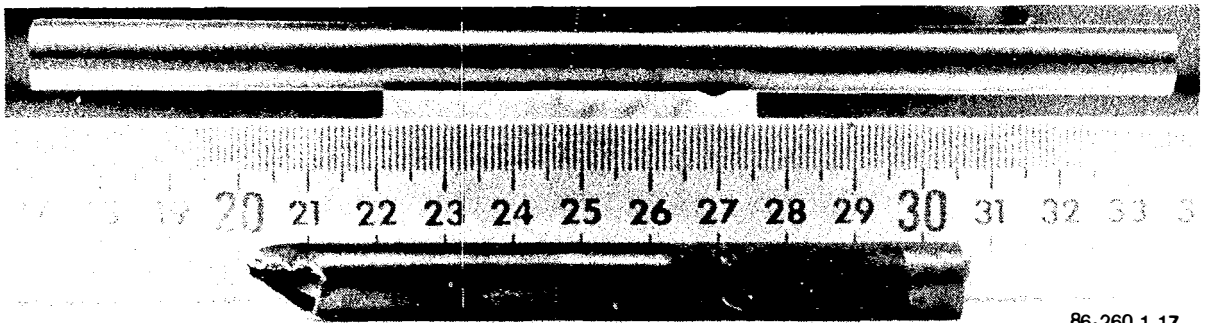
86-260-2-7

Figure 30. View of Segment 5, showing the top end deformed by the TMI-2 defueling shear tool. A new segment of fuel rod cladding is shown at the left for comparison.



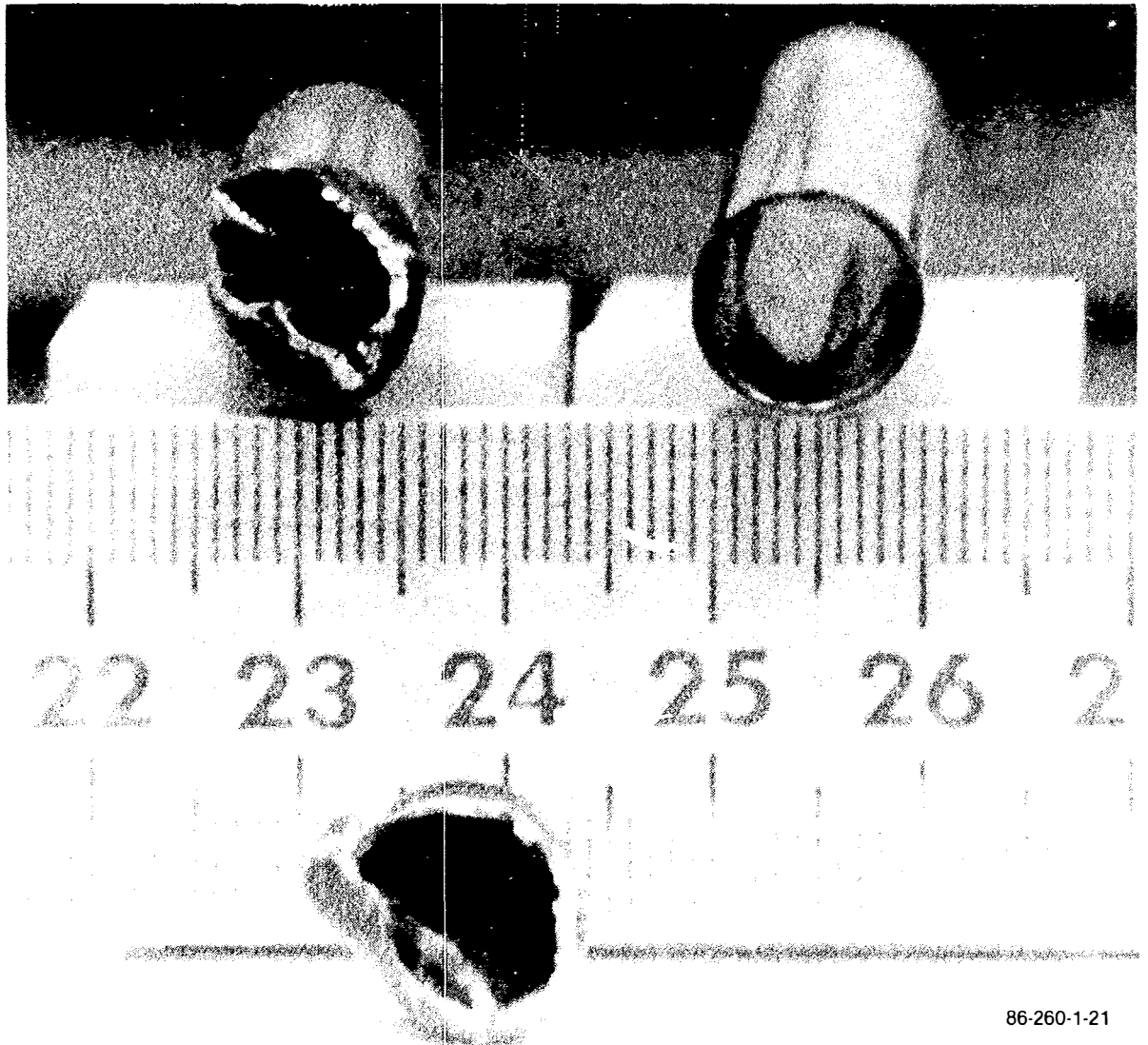
86-260-2-8

Figure 31. View of Segment 5, showing the bottom end deformed by the TMI-2 defueling shear tool. A new segment of fuel rod cladding is shown at the left for comparison.



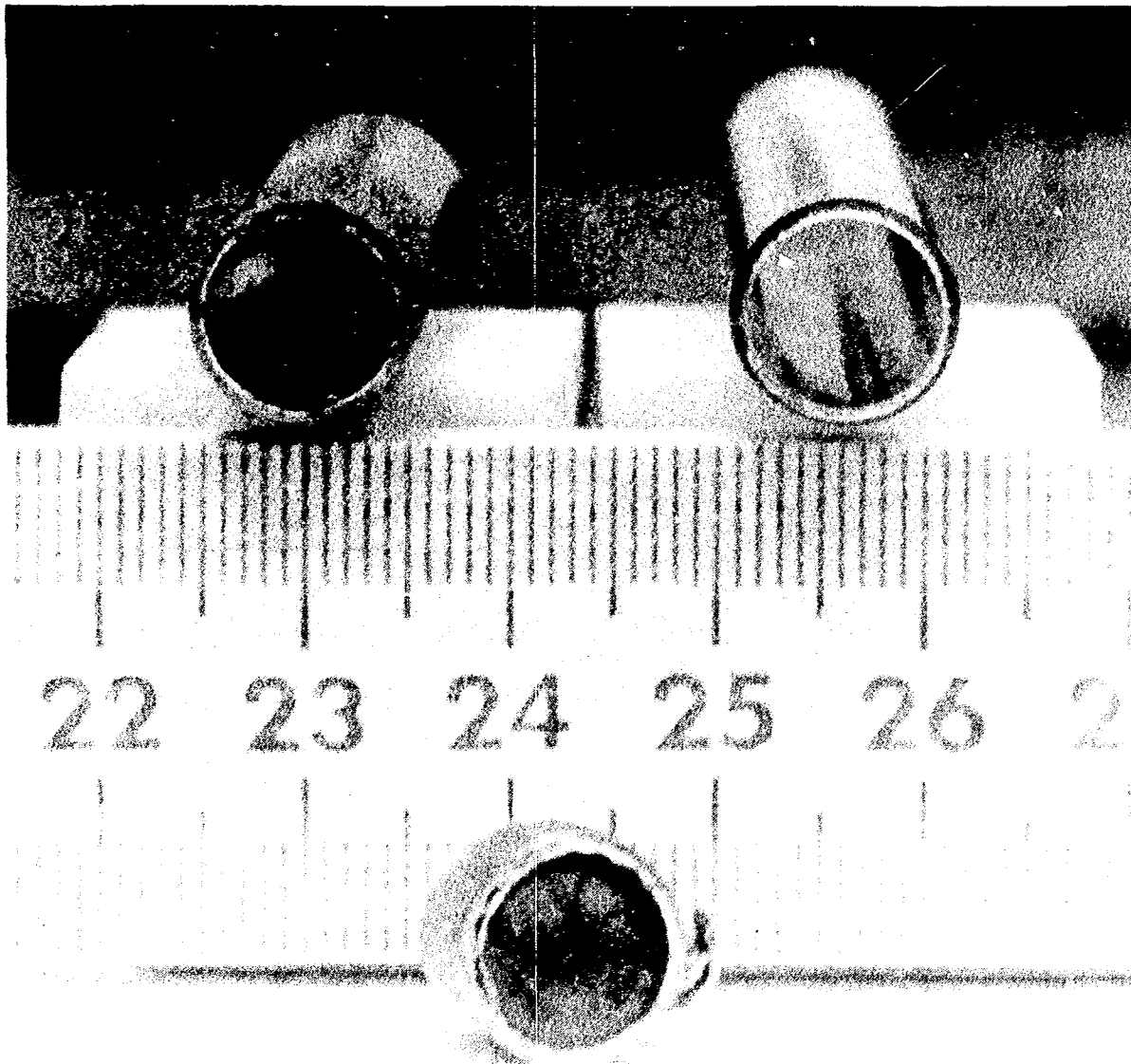
86-260-1-17

Figure 32. Side view of Segment 6, after sectioning removal of the lower end deformed by the TMI-2 defueling shear tool. A new segment of fuel rod cladding is shown above for comparison.



86-260-1-21

Figure 33. View of Segment 6, showing the top end deformed by the TMI-2 defueling shear tool. The removed end is shown below, and a new segment of fuel rod cladding is shown at the right for comparison.



86-260-1-22

Figure 34. View of Segment 6, after sectioning removal of the bottom end deformed by the TMI-2 defueling shear tool. The removed end is shown below, and a new segment of fuel rod cladding is shown at the right for comparison.

## 5. OBSERVATIONS/CONCLUSIONS

The following observations have been made concerning the six fuel rod segments:

- Neutron radiographs of the segments show some evidence of possible pellet/cladding interaction.
- The gamma spectroscopy analysis results agree with the ORIGEN2 calculated concentration values within the uncertainty of the analysis, except for retention of Eu-154, which is lower than expected. This is an expected result, as Eu-154 cannot be predicted with a high degree of accuracy.
- Segment 1 appears to have been flattened in the region where fuel pellets may have fallen out of the open end during the accident. There is no evidence of shearing or handling that could have caused the deformation.
- There is no evidence of significant zircaloy oxidation on any of the rod segments, indicating these fuel rod regions did not get hot enough (>1500 K) to be subjected to oxidation during the accident.
- The TMI-2 fuel rods used zircaloy sleeve spacers between the pellet stack holddown springs and fuel pellets instead of the expected  $ZrO_2$  washers (see Table 1), as determined from the neutron radiographs.
- No evidence of prior molten materials was observed in any of the segments.

The segments analyzed present examples of intact rod sections or rods where pellets have fallen out and the cladding flattened, possibly during the accident. Destructive examination of these samples was not recommended by the TMI-2 Accident Evaluation Program because other fuel rod segments

became available which were subjected to higher temperatures and which contained interaction zones between components. These fuel rod segment samples were, however, distributed to other national laboratories and to European countries as part of domestic and international TMI-2 examination programs.

## 6. REFERENCES

1. N. Rogovin, Three Mile Island: A Report to the Commissioners and to the Public, U.S. Nuclear Regulatory Commission Report, NUREG/CR 1250.
2. E. L. Tolman et al., TMI-2 Accident Evaluation Program, EGG-TMI-7048, February 1986.
3. TMI-2 Accident Core Heat-Up Analysis, NSAC-25, Nuclear Associates International and Energy Incorporated, June 1981.
4. L. S. Beller and H. L. Brown, Design and Operation of the Core Topography Data Acquisition System for TMI-2, GEND-INF-012, May 1984.
5. K. Vinjamuri et al., Examination of H8 and B8 Leadscrews from Three Mile Island Unit 2, GEND-INF-052, September 1985.
6. J. E. Klein, M. H. Putnam, R. H. Helmer, GAUSS VI, A Computer Program for the Automatic Analysis of Gamma Rays from Germanium Spectrometers, ANRC-13, June 1973.
7. B. G. Schnitzler and J. B. Briggs, TMI-2 Isotopic Inventory Calculations, EGG-PBS-6798, August 1985.

**APPENDIX A**  
**GAMMA SPECTROSCOPY ANALYSIS RESULTS**

## APPENDIX A

### GAMMA SPECTROSCOPY ANALYSIS RESULTS

This appendix presents the geometry and calibration methods and results of the gamma spectroscopy analysis of the intact fuel rod segments. The geometry used for the fuel rod segment measurement is shown in Figure A-1. Two collimators were used, the second collimator located adjacent to the fuel rod segment. This method allows measurements of 1-cm increments of the fuel rod. The detector collimator 1 and the fuel rod segment were aligned by taking a series of measurements at different detector heights to determine the optimum source-to-detector alignment. All measurements were performed without modifying this alignment.

To perform measurements at different rod locations, each fuel rod was attached to a scanning bed which could be translated passed collimator No. 2 in 1-cm increments.

Calibration of the measurement system was performed using a simulated fuel rod segment containing 952  $\mu\text{Ci}$  of Eu-152. The uncertainty associated with this standard is approximately 30%, owing to density and activity variations in the standard. Table A-1 presents the measured count rates obtained at various locations along the standard. These data were integrated, and an efficiency curve was generated (i.e., counts/gamma) (Table A-2).

Table A-3 lists the measured radionuclide data in counts per second for Segment 5 (core position M2, rod position R13). Eighteen measurements were taken along the length of this segment to define the fission product distribution within the rod segment.

Table A-4 presents the measured radionuclide count rate data for Segments 1, 2, 3, 4, and 6.

Table A-5 lists the calculated counts per gamma efficiencies for each radionuclide at the energies characteristic of each radionuclide measurable in the fuel rod segments.

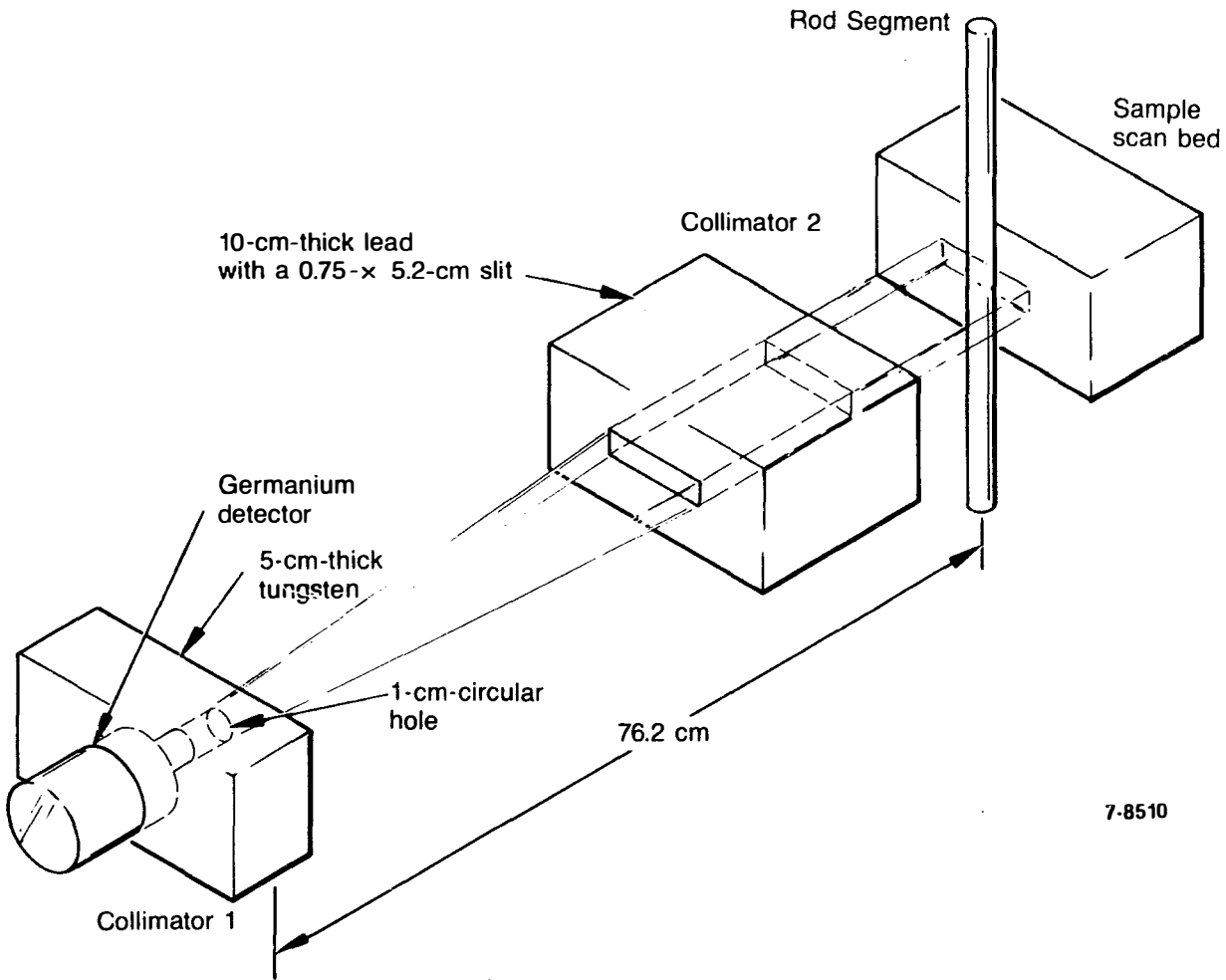


Figure A-1. Gamma spectrometry system configuration.

TABLE A-1. CALIBRATION MEASUREMENTS USING THE EUROPIUM-152 STANDARD<sup>a</sup>  
(counts/s  $\pm$  1  $\sigma$  in %)

Energy (KeV)	Axial Distance from Center of Standard							
	3 cm Left <sup>b</sup>	2 cm Left <sup>c</sup>	1 cm Left <sup>c</sup>	Center <sup>b</sup>	Center <sup>c</sup>	1 cm Right <sup>c</sup>	2 cm Right <sup>c</sup>	3 cm Right <sup>b</sup>
244.70	0.202 $\pm$ 26	0.184 $\pm$ 20	0.837 $\pm$ 6.0	0.861 $\pm$ 6	0.970 $\pm$ 6.1	1.33 $\pm$ 4.5	1.13 $\pm$ 5	0.308 $\pm$ 26
344.28	1.60 $\pm$ 2.8	2.81 $\pm$ 3.4	7.32 $\pm$ 2.2	7.99 $\pm$ 1.1	8.20 $\pm$ 1.1	11.1 $\pm$ 2.3	10.90 $\pm$ 1.6	2.54 $\pm$ 2.7
443.98	0.307 $\pm$ 11	0.503 $\pm$ 9.5	1.23 $\pm$ 4.8	1.19 $\pm$ 3.8	1.27 $\pm$ 6.5	1.79 $\pm$ 3.1	1.62 $\pm$ 3	0.389 $\pm$ 10
778.91	1.03 $\pm$ 5.9	2.01 $\pm$ 3.7	4.82 $\pm$ 1.7	4.95 $\pm$ 1.4	5.07 $\pm$ 3.4	7.12 $\pm$ 1.7	6.56 $\pm$ 1.3	1.53 $\pm$ 4.3
867.39	0.312 $\pm$ 9.1	0.663 $\pm$ 5.0	1.42 $\pm$ 3.2	1.63 $\pm$ 2.9	1.58 $\pm$ 3.0	2.21 $\pm$ 4.1	2.09 $\pm$ 2.6	0.468 $\pm$ 6.5
964.13	1.11 $\pm$ 3.3	2.28 $\pm$ 2.2	5.02 $\pm$ 2.3	5.10 $\pm$ 1.4	5.44 $\pm$ 2.1	7.67 $\pm$ 1.1	6.52 $\pm$ 2.0	1.61 $\pm$ 2.7
1085.91	0.737 $\pm$ 4.9	1.63 $\pm$ 2.9	3.37 $\pm$ 2.2	3.46 $\pm$ 1.7	3.59 $\pm$ 1.7	5.08 $\pm$ 1.4	4.48 $\pm$ 2.1	1.07 $\pm$ 3.3
1112.12	0.955 $\pm$ 3.5	2.05 $\pm$ 2.2	4.35 $\pm$ 2.2	4.71 $\pm$ 1.4	4.89 $\pm$ 2.7	7.02 $\pm$ 1.9	5.84 $\pm$ 2.8	1.34 $\pm$ 2.9
1408.01	1.31 $\pm$ 3.5	2.98 $\pm$ 1.7	6.20 $\pm$ 1.9	6.70 $\pm$ 3.1	6.84 $\pm$ 2.0	9.28 $\pm$ 1.4	8.00 $\pm$ 1.3	1.87 $\pm$ 2.2

a. Dimensions of the standard:

Cladding OD = 1.1 cm  
 Cladding ID = 0.98 cm  
 Cladding length = 7.6 cm  
 Lead = 6.3 cm x 0.9 cm (diameter)  
 Hole in lead = 3.30 cm (length)  
 Volume of hole = 0.37 mL  
 Length of Eu-152 source = 5.07 cm

b. Measurements obtained on May 15, 1986.

c. Measurements obtained on May 14, 1986.

TABLE A-2. CALIBRATION EFFICIENCY DATA

---

<u>Energy (KeV)</u>	<u>Relative Intensity (gammas/disintegration)</u>	<u>Total counts/s<sup>a</sup></u>	<u>Efficiency (counts/gamma)</u>
244.70	8	4.706	1.67 E-6
344.28	27	41.90	4.41 E-6
443.98	4	6.76	4.80 E-6
778.91	14	26.86	5.45 E-6
867.39	4	8.30	5.89 E-6
964.13	15	28.29	5.36 E-6
1085.91	12	19.05	4.50 E-6
1112.12	14	25.30	5.13 E-6
1408.01	22	34.89	4.50 E-6

---

a. Total activity = 952  $\mu$ Ci or 3.52 E+7 disintegrations/s

---

TABLE A-3. GAMMA SPECTROSCOPY DATA FOR SEGMENT 5<sup>a</sup>  
(counts/s  $\pm$  1  $\sigma$  in %)

Measurement	Radionuclide						
	Cs-137	Cs-134 <sup>b</sup>	Sb-125	Ru-106	Ce-144	Eu-154	Co-60
1	2135 $\pm$ 3	13.75 $\pm$ 6	11.16 $\pm$ 6	6.33 $\pm$ 5.5	2.23 $\pm$ 7	0.596 $\pm$ 9	4.64 $\pm$ 2.6
2	2642 $\pm$ 3	15.86 $\pm$ 10	13.63 $\pm$ 10	7.50 $\pm$ 5.32	3.10 $\pm$ 15	0.787 $\pm$ 9	4.62 $\pm$ 3.5
3	2577 $\pm$ 3	16.27 $\pm$ 9	13.14 $\pm$ 5	7.07 $\pm$ 4.5	2.36 $\pm$ 10	0.662 $\pm$ 10.4	4.73 $\pm$ 2.3
4	2501 $\pm$ 2.8	15.20 $\pm$ 10.4	13.83 $\pm$ 15	6.26 $\pm$ 6.8	2.87 $\pm$ 9.7	0.692 $\pm$ 10	4.99 $\pm$ 2.2
5	2450 $\pm$ 3.1	14.85 $\pm$ 10.8	12.94 $\pm$ 8.4	7.17 $\pm$ 5.7	2.57 $\pm$ 7	0.751 $\pm$ 9.4	4.84 $\pm$ 2.3
6	2389 $\pm$ 3.1	13.58 $\pm$ 12.4	13.96 $\pm$ 10.5	6.90 $\pm$ 5.4	2.57 $\pm$ 13.2	0.584 $\pm$ 10.3	4.65 $\pm$ 2.3
7	2312 $\pm$ 3.2	12.60 $\pm$ 11.7	13.10 $\pm$ 15	6.31 $\pm$ 9.2	2.30 $\pm$ 15.5	0.587 $\pm$ 12	4.58 $\pm$ 2.3
8	2244 $\pm$ 3.1	12.05 $\pm$ 11	12.90 $\pm$ 17.3	6.31 $\pm$ 5.1	2.48 $\pm$ 8.3	0.452 $\pm$ 12	4.78 $\pm$ 2.3
9	2169 $\pm$ 3.2	11.60 $\pm$ 7.1	12.77 $\pm$ 4.5	5.92 $\pm$ 6.3	2.03 $\pm$ 8.3	0.531 $\pm$ 12	4.72 $\pm$ 2.3
10	2092 $\pm$ 3.3	10.67 $\pm$ 7.9	10.64 $\pm$ 10.2	6.34 $\pm$ 10.7	2.87 $\pm$ 10.5	0.452 $\pm$ 12.5	4.68 $\pm$ 2.2
11	2016 $\pm$ 3.1	10.03 $\pm$ 7.7	11.78 $\pm$ 11	5.91 $\pm$ 7	1.90 $\pm$ 7.4	0.538 $\pm$ 11.7	4.62 $\pm$ 2.2
12	1894 $\pm$ 1.6	9.67 $\pm$ 7.3	10.44 $\pm$ 6.6	5.56 $\pm$ 15	1.95 $\pm$ 7.3	0.399 $\pm$ 13.3	4.61 $\pm$ 2.2
13	1826 $\pm$ 1.6	9.46 $\pm$ 9.9	6.33 $\pm$ 35	5.33 $\pm$ 7.1	1.88 $\pm$ 6.9	0.424 $\pm$ 12.6	4.60 $\pm$ 2.5
14	1765 $\pm$ 1.6	8.58 $\pm$ 18	10.22 $\pm$ 4.7	5.44 $\pm$ 13	1.97 $\pm$ 7.5	0.391 $\pm$ 21.4	4.77 $\pm$ 2.1
15	1702 $\pm$ 1.5	7.67 $\pm$ 8.7	10.59 $\pm$ 10	5.14 $\pm$ 15	1.78 $\pm$ 7.2	0.269 $\pm$ 15.5	4.65 $\pm$ 2.9
16	1443 $\pm$ 1.3	4.10 $\pm$ 27	9.64 $\pm$ 8.8	4.28 $\pm$ 4.9	1.50 $\pm$ 8.1	0.457 $\pm$ 21	4.63 $\pm$ 2.1
17	571 $\pm$ 5.7	2.27 $\pm$ 24	3.766 $\pm$ 6.8	2.03 $\pm$ 14	0.663 $\pm$ 10.3	0.136 $\pm$ 20	4.34 $\pm$ 3.5
18	27.1 $\pm$ 3.3	0.245 $\pm$ 45	--	--	--	--	4.50 $\pm$ 2.9

9-A-6

a. Core position M2, rod position R13, upper segment.

b. Cs-134 included for comparison only.

TABLE A-4. GAMMA SPECTROSCOPY DATA FOR SEGMENTS 1, 2, 3, 4, AND 6  
(counts/s  $\pm$  1  $\sigma$  in %)

Measurement	Location	Radionuclide						
		Sb-125	Cs-134	Ru-106	Cs-137	Ce-144	Eu-154	Co-60
Segment 1 (core position L1, rod position B10, lower segment)								
1	3 cm from bottom of fuel	9.17 $\pm$ 2.4	1.49 $\pm$ 39	--	61.7 $\pm$ 1.5	--	--	4.67 $\pm$ 1.01
2	7 cm from bottom of fuel	28.5 $\pm$ 12	54.1 $\pm$ 4	15.8 $\pm$ 10	4790 $\pm$ 3	5.68 $\pm$ 9	2.70 $\pm$ 6	4.85 $\pm$ 5
3	11 cm from bottom	25.2 $\pm$ 21	42.1 $\pm$ 7	12.2 $\pm$ 5	3930 $\pm$ 3	4.89 $\pm$ 11	2.06 $\pm$ 5	5.09 $\pm$ 3
4	14 cm from bottom	22.4 $\pm$ 7	44.3 $\pm$ 6	13.8 $\pm$ 7	4330 $\pm$ 3	5.34 $\pm$ 7	2.02 $\pm$ 8	4.94 $\pm$ 5
5	16 cm from bottom	20.6 $\pm$ 11	33.1 $\pm$ 8	10.9 $\pm$ 12	3440 $\pm$ 3	3.39 $\pm$ 15	1.51 $\pm$ 7	4.73 $\pm$ 4
Segment 2 (core position L1, rod position B10, upper segment)								
1	1 cm from bottom	11.9 $\pm$ 5.2	13.6 $\pm$ 7.5	6.09 $\pm$ 5.1	1974 $\pm$ 15	1.89 $\pm$ 8.8	0.548 $\pm$ 9.4	4.59 $\pm$ 3.3
2	3 cm from bottom	15.5 $\pm$ 8.4	16.8 $\pm$ 5.9	8.53 $\pm$ 6.4	2638 $\pm$ 3.6	2.94 $\pm$ 8.2	0.770 $\pm$ 8.6	6.41 $\pm$ 3.4
3	7 cm from bottom	6.71 $\pm$ 38	10.8 $\pm$ 12	5.35 $\pm$ 4.8	2077 $\pm$ 3.2	2.05 $\pm$ 9.3	0.534 $\pm$ 10	4.84 $\pm$ 3.4
4	10.5 cm from bottom	8.72 $\pm$ 12	7.89 $\pm$ 8.0	4.82 $\pm$ 4.7	1808 $\pm$ 3.0	1.90 $\pm$ 7.2	0.376 $\pm$ 13	4.69 $\pm$ 2.2
5	2 cm from top (spring)	3.74 $\pm$ 4.6	0.61 $\pm$ 37	--	40.3 $\pm$ 20	--	0.27 $\pm$ 13	4.64 $\pm$ 2.2
Segment 3 (core position N2, rod position N1)								
1	2 cm from bottom	11.1 $\pm$ 15	7.74 $\pm$ 10	4.60 $\pm$ 12	1700 $\pm$ 3	1.64 $\pm$ 7	0.275 $\pm$ 15	4.64 $\pm$ 4
2	4 cm from bottom	8.92 $\pm$ 5	6.41 $\pm$ 12	4.71 $\pm$ 7	1570 $\pm$ 3	1.60 $\pm$ 7	0.290 $\pm$ 14	4.43 $\pm$ 3
3	7 cm from bottom	9.11 $\pm$ 11	2.64 $\pm$ 26	3.78 $\pm$ 5	1340 $\pm$ 2	1.16 $\pm$ 8	0.153 $\pm$ 23	4.53 $\pm$ 3
4	10 cm from bottom	4.75 $\pm$ 34	2.34 $\pm$ 27	3.03 $\pm$ 18	1200 $\pm$ 2	1.34 $\pm$ 8	0.143 $\pm$ 20	4.48 $\pm$ 2
5	13.5 cm from bottom	3.05 $\pm$ 4	0.843 $\pm$ 27	--	15.6 $\pm$ 2	--	--	4.44 $\pm$ 3
Segment 4 (core position M2, rod position R15)								
1	1 cm from bottom	13.4 $\pm$ 5	14.5 $\pm$ 6	6.27 $\pm$ 7	2215 $\pm$ 1.4	2.31 $\pm$ 6.6	0.652 $\pm$ 8.7	4.80 $\pm$ 2.2
2	3 cm from bottom	14.0 $\pm$ 8.4	16.6 $\pm$ 8.7	7.48 $\pm$ 4.1	2589 $\pm$ 3.6	2.56 $\pm$ 12	0.590 $\pm$ 11	4.84 $\pm$ 2.9
3	Center	11.9 $\pm$ 7.3	11.8 $\pm$ 9.4	6.20 $\pm$ 6.5	2160 $\pm$ 3.4	2.21 $\pm$ 7.5	0.474 $\pm$ 13	4.80 $\pm$ 2.2
4	1 cm from top	6.8 $\pm$ 10	2.41 $\pm$ 2.6	2.48 $\pm$ 13	818 $\pm$ 1.4	0.727 $\pm$ 13	0.178 $\pm$ 15	4.61 $\pm$ 2.1
5	3 cm from top	5.5 $\pm$ 50	7.37 $\pm$ 9.7	5.25 $\pm$ 4.8	1705 $\pm$ 2.9	1.66 $\pm$ 13	0.252 $\pm$ 17	4.68 $\pm$ 2.2

TABLE A-4. (continued)

Measurement	Location	Radionuclide						
		Sb-125	Cs-134	Ru-106	Cs-137	Ce-144	Eu-154	Co-60
Segment 6 <sup>a</sup> (core position M2, rod position R13, lower segment)								
1	1 cm from bottom	13.9 ± 8.4	19.4 ± 9.1	7.57 ± 4	2482 ± 2.5	2.67 ± 9.3	0.770 ± 13	4.77 ± 2.9
2	3 cm from bottom	15.6 ± 4.1	22.2 ± 8.6	8.60 ± 4.9	3070 ± 3.6	3.49 ± 13	1.11 ± 8.1	4.28 ± 5.1
3	Center	9.33 ± 41.	21.4 ± 10	9.97 ± 6.0	2959 ± 3.6	2.96 ± 12	0.903 ± 8.9	4.80 ± 2.5
4	1 cm from top	4.42 ± 6.3	3.23 ± 10	1.79 ± 7.5	481 ± 0.7	0.55 ± 20	0.175 ± 16	4.54 ± 2.1
5	3 cm from top	14.9 ± 6.7	18.0 ± 8.3	7.82 ± 4.6	2724 ± 3.0	2.83 ± 7.7	0.894 ± 9.1	4.83 ± 3.9

a. For reference, background measured activities for Segment 6 were as follows:

Cs-137 = 1.17 ± 2.3  
Cs-134 = 0.062 ± 10  
Co-60 = 4.27 ± 0.9

TABLE A-5. INDIVIDUAL RADIONUCLIDE EFFICIENCIES AT DEFINED ENERGIES

---

<u>Radionuclide</u>	<u>Energy<sup>a</sup> (KeV)</u>	<u>Efficiency<sup>b</sup> (counts/gamma)</u>
<sup>137</sup> Cs	661.7	5.22 E-6
<sup>125</sup> Sb	427.9	4.74 E-6
<sup>106</sup> Ru	621.8	5.15 E-6
<sup>144</sup> Ce	696.5	5.29 E-6
<sup>154</sup> Eu	1274	4.79 E-6
<sup>60</sup> Co	1332	4.66 E-6

---

a. The energies used for isotope analysis re the principal energies (i.e., largest branching ratio) for these radionuclides or are the highest without interferences.

b. Efficiency is determined by interpolating between measured calibration points.

---